UCLouvain

École polytechnique de Louvain

How can carbon capture utilisation and storage help decarbonising the port of Antwerp?

Author: **Louis Dubucq**
Supervisors: **Francesco Contino**, **Diederik Coppitters**, **Xavier Rixhon**
Reader: **Patricia Luis Alconero**
Academic year 2022–2023
Master [120] in Mechanical Engineering

Acknowledgements

Everything started in Melbourne where I met Arthur Johnson, a truly amazing friend. Real source of inspiration, he wrote articles, has already founded Picks, and adds up the professional experiences, at only 21 years old. He gave me confidence in my English skills and revised the text of this thesis.

Based on EnergyScope Typical Days, I would like to thank Gauthier Limpens for its masterpiece thesis and everyone who contributed and continues to contribute to the development of this model.

This thesis would not be possible without the help of Diederik Coppitters who supervised me throughout the year. He gave me insightful advice and remarks that I will carry for my future projects. His commitment and flexibility for our frequent meetings are remarkable. He stimulated me until the end and highlighted my strengths.

Thanks also to Xavier Rixhon who helped me to understand and to decipher EnergyScope Typical Days. He gave me fantastic ideas for the implementation.

Naturally, I would like to express my gratefulness to Patricia Luis Alconero, member of the jury.

Special thanks to Professor Francesco Contino who first raised my curiosity about climate change a few years ago. Beyond being a brilliant teacher, he inspired me and fostered my attention to detail.

I would like to thank Victor Somville with whom we spent hours working together on our respective thesis. When he was not boosting me up during our sport sessions, he was listening to my problems and my concerns about this thesis.

Finally, I would like to give a huge thanks to my family. They supported me mentally throughout my academic career.

Special thoughts to Leon Gillieaux, the shining star in the dark sky.

Abstract

The port of Antwerp is vital for the Belgian economy. This port provides jobs for more than 150,000 people and is ranked as the biggest chemical cluster of Europe. However, its industrial activities also release significant GreenHouse Gases (GHG). In response to the emissions mitigation target of Belgium for 2030 (-47% compared to 2005), the project Antwerp@C has come to life. Its goal is to halve the CO_2 emissions of the port by 2030 and to reach net zero in 2050 by means of Carbon Capture Utilisation (CCU) and Storage (CCS). In this context, this thesis aims to analyse the economic feasibility and the impacts on the Belgian energy system in 2030, when the captured CO_2 of the port is used for Power-to-Gas (PtG) and/or stored.

In this study, the technologies making up a PtG system are first reviewed. The characteristics of each of these technologies are then determined in accordance to the Antwerp@C project. After, the estimation of the CO_2 emissions of the port of Antwerp and the future hydrogen availability for the methanation is described. The energy model used as well as the method for the economic analysis, and the sensitivity analysis are also detailed.

The results outline that the port is responsible for 15.9–18.8% of the total CO_2 emissions of Belgium in 2019 (90.2 Mt_{CO_2}). In terms of installed capacities of the technologies generating electricity, utilising all the captured CO_2 to produce Synthetic Natural Gas (SNG) is unrealistic, despite a relatively small total cost for the system (1.2% of Belgian gross domestic product). Using only part of the captured CO_2 and permanently storing the rest represent a more feasible scenario. In this scenario, consuming the estimated quantity of hydrogen, projected to be available for methanation in 2030, results in 16.3–41.6% of captured CO_2 used and the rest is stored. The range represents the uncertainty in the amount of captured CO_2 and H_2 used. Finally, the levelised cost of synthetic natural gas (LCSNG) covers a range from 40.7 $€_{2015}$/MWh to 734.1 $€_{2015}$/MWh, depending on the electricity price, the carbon price and the CO_2 capture technology used. Considering the uncertainty associated with these parameters, PtG becomes economically attractive for electricity prices between 41 €/MWh and 50 €/MWh by assuming a price of the SNG of 75 €/MWh.

Contents

Nomenclature

List of abbreviations

AE	Alkaline Electrolyser
ASU	Air Separation Unit
CAPEX	Capital Expenditure
CCGT	Combined Cycle Gas Turbine
CCS	Carbon Capture and Storage
CCU	Carbon Capture and Utilisation
CEPCI	Chemical Engineering Plant Cost Index
CHP	Combined Heat and Power
CPU	Compression and Purification Unit
DHN	District Heating Network
E-PRTR	European Pollutant Release and Transfer Register
ESTD	EnergyScope Typical Days
FGPU	Flue Gas Processing unit
GHG	GreenHouse Gas
GID	Global Infrastructure emission Database
GWP	Global Warming Potential
HVC	High-Value Chemicals
LCOE	Levelised Cost of Energy
LCSNG	Levelised Cost of Synthetic Natural Gas

LHV	Lower Heating Value
MEA	Monoethanolamine
OPEX	Operational Expenditure
PEME	Proton Exchange Membrane Electrolyser
PtG	Power-to-Gas
PV	Photovoltaic
SNG	Synthetic Natural Gas
SOE	Solid Oxide Electrolyser

List of figures

Chapter D: Results for oxy-fuel combustion capture

List of tables

Chapter 1

Introduction

Climate change is the biggest challenge humans have ever faced. The global-mean temperature has already surpassed 1.1°C. The consequences are visible around the globe with more intense and frequent extreme weather such as fires, floods, droughts, etc. The latest report of the International Panel on Climate Change (IPCC) makes it clear that the cause is the anthropogenic Greenhouse Gas (GHG) emissions [1]. In response to this urging situation, 194 Parties ratified the Paris Agreement to limit the temperature increase to 2°C and to keep on their efforts to achieve 1.5°C [2].

As a result of the Agreement, the Belgium's government decided to mitigate emissions of -47% in 2030 compared to 2005. In 2020, Belgium emitted 82.7 Mt_{CO_2}; of which 23 Mt_{CO_2} come from industries [3]. Carbon Capture Utilisation (CCU) and Storage (CCS) stand among the tools in the toolbox to decarbonise those industries. CCU and CCS are especially attractive in industrial clusters, as sharing infrastructures reduces the costs through economies of scale, and limits the investment risks [4].

Among the CO_2 utilisation options, Power-to-Gas (PtG) or Power-to-Liquid (PtL) offer several advantages. PtG and PtL are defined as follows. On the one side, hydrogen is produced by water electrolysis with surplus of electricity. On the other side, CO_2 is captured either from flue gases or from the air, and is then combined to produce Synthetic Natural Gas (SNG) or a liquid (e.g. methanol). With the rising need for flexibility due to the intermittent renewable energy, they are part of the portfolio to absorb peak electricity production with other forms of electricity storage.

In this study, the production of SNG by PtG has been selected for two main reasons. First, as Belgium has planned to phase out nuclear power, new gas turbines are required to be built in order to ensure the security of the electricity supply. Second, gas infrastructures and network are highly developed.

The port of Antwerp, the biggest industrial cluster of Belgium, is crucial for the Belgian economy as it represents more than 150,000 jobs, and is the biggest chemical hub of Europe [5]. In response to the emissions reduction target of Belgium, the project Antwerp@C aims to halve

emissions of the port by 2030 and to be carbon neutral by 2050, using CCU and CCS [6].

Novelty. The goal of this thesis is to analyse the economic feasibility and the impacts of PtG with CO_2 captured from the industries of the port of Antwerp and of CO_2 storage on the energy system, to reach Belgium's objective of halving emissions by 2030.

First, a review of the technologies constituting the PtG system is conducted (i.e. the CO_2 capture, the electrolyser, the methanation unit and the CO_2 storage). Each review is followed by the determination of the specific characteristics of the corresponding technology. Second, the quantification of the two main inputs of PtG (H_2 and CO_2) is detailed. Then, the energy model used to obtain the results is described and the method for the economic analysis and the sensitivity analysis is explained. Finally, the results are analysed in Chapter 3.

Chapter 2

Methodology

This chapter starts with a review and the determination of each technology making up the PtG system (Sections 2.1, 2.2, 2.3 and Section 2.4). The focus is then set on the method followed to estimate the two main inputs of the system: CO_2 and H_2 (Sections 2.5 and 2.6). Next, the energy model used to obtain a snapshot of the Belgian energy system in 2030 is described (Section 2.7). Finally, the methodology of the economic and the sensitivity analysis is explained (Sections 2.8 and 2.9).

2.1 CO_2 capture

There are three different strategies to capture CO_2 from stationary point sources: pre-combustion, post-combustion and oxy-fuel combustion capture [7]. These strategies are combined with CO_2 separation technologies to separate the CO_2 from the flue gas. Once the CO_2 is separated from the other gases, the CO_2 is compressed and further purified, if necessary, in the CO_2 Compression and Purification Unit (CPU). The CO_2 meets then the quality requirements to be transported in the pipelines for further storage and/or utilisation. In this section, an overview of the different CO_2 capture and separation technologies will be presented based on a literature review. Their advantages and drawbacks are summarised in Tables 2.1 and 2.2, respectively.

2.1.1 State of the art: CO_2 capture strategies

Pre-combustion capture

The pre-combustion capture consists in processing the fuel before the combustion to produce two separate streams of hydrogen and carbon dioxide (Figure 2.1). The hydrogen can then be used as the fuel. This process is divided into two main steps. First, the fuel reacts with steam or oxygen, in which case the reaction is called “steam reforming” and “partial oxidation”, respectively [8, 9]. Depending on the type of application and design choices, one of the two reactions is chosen. Combining these two reactions is also possible and is called “authotermal reforming ”[9].

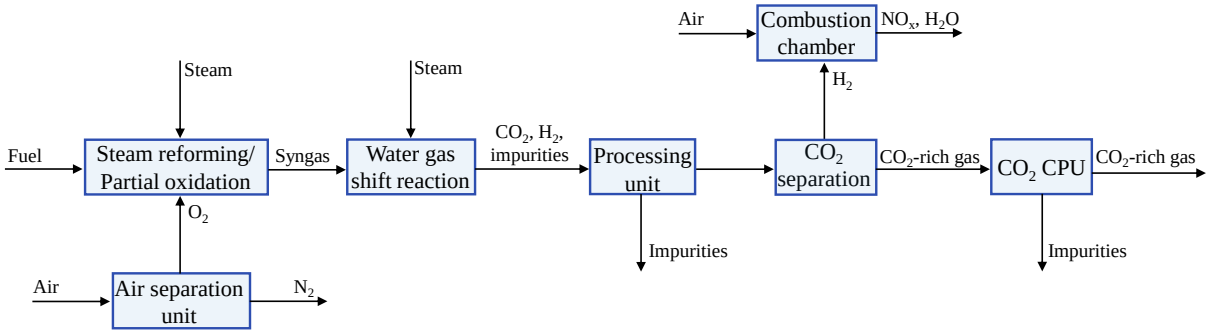

Figure 2.1: Flow chart of the pre-combustion capture.

$$\begin{aligned} C_xH_y + xH_2O &\rightleftharpoons xCO + \left(x + \frac{y}{2}\right)H_2 \quad \textbf{(steam reforming)} \\ C_xH_y + \frac{x}{2}O_2 &\rightleftharpoons xCO + \left(\frac{y}{2}\right)H_2 \quad \textbf{(partial oxidation)} \end{aligned} \tag{2.1}$$

When partial oxidation is carried out, the source of oxygen is produced with an Air Separation Unit (ASU) which significantly increases the costs and the energy requirement[1]. Then, the carbon monoxide in the syngas is converted into CO_2 using steam by the water gas shift reaction.

$$CO + H_2O \rightleftharpoons CO_2 + H_2 \quad \textbf{(water gas shift reaction)} \tag{2.2}$$

This mixture of CO_2 and H_2 has a CO_2 concentration of roughly 15–60%vol on a dry basis according to Allam *et al.* [9]. Finally, the CO_2 is separated from the H_2 by one of the gas separation techniques detailed in Section 2.1.2. Depending on the fuel used and the level of purity of the products required, additional units may be necessary to remove the impurities, such as nitrogen, ash or sulfur oxides [9, 10].

Using the produced hydrogen as a fuel is the main advantage of this capture system, as it does not produce CO_2. [8]. Moreover, the efficiency of the gas separator is improved due to the higher CO_2 concentration compared to the combustion without a capture system [7]. However, this capture strategy has high investments and operating costs due to the additional units and the complexity of the process [7, 11]. Consequently, retrofitting an existing plant is laborious and onerous.

Post-combustion capture

The process of removing the CO_2 in the flue gas produced by the combustion is called post-combustion capture. Before being vented in the air, the flue gas passes through a CO_2 separation technology whose fundamentals are reviewed in Section 2.1.2. Before separating the

[1] More information about the ASU is provided in Section 2.1.1

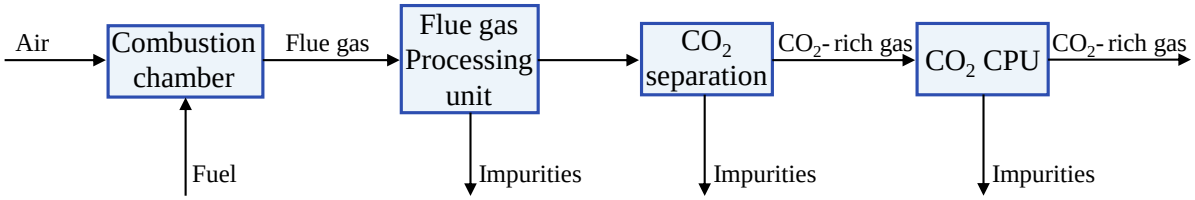

Figure 2.2: Flow chart of the post-combustion capture.

CO_2 from the flue gas, additional features eliminate the impurities, such as SO_x, NO_x, particulate matter and water so as to avoid corrosion. For this purpose, a Flue Gas Processing Unit (FGPU) composed of units, such as a $DeNO_x$ unit, an electrostatic precipitator for ash removal and/or a desulphurisation unit, treats the flue gas to comply with the quality requirement of the following units (Figure 2.2). The flue gas is also cooled down to meet the thermal constraints of the CO_2 separation techniques.

As the CO_2 concentration ranges from 3%vol to 14%vol (dry basis) after a combustion [9], a significant amount of energy is required to separate the CO_2 and reach a high-concentrated CO_2 stream begetting large energy costs too. On the other side, post-combustion capture has the benefit of easily retrofitting existing facilities. In fact, only small changes need to be applied. Therefore, post-combustion stands as the best retrofit option among the two other approaches [7, 12]. This method has also the benefit of being the most mature CO_2 capture technology [7, 8, 11].

Oxy-fuel combustion capture

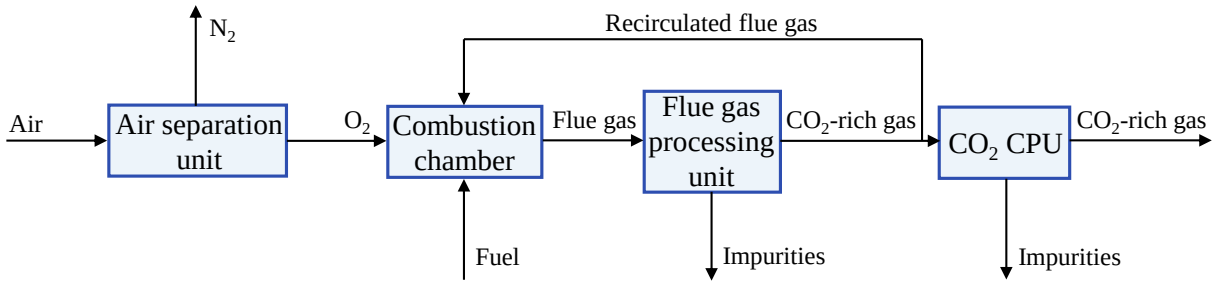

Figure 2.3: Flow chart of the oxy-fuel combustion capture.

Oxy-fuel combustion capture refers to burning the fuel with oxygen instead of air. This results in a complete[2] combustion whose the flue gas contains mainly CO_2 and H_2O. Therefore, the CO_2 separation is significantly simplified, as this step is performed by condensing the

[2]In reality, the mixture of the oxygen with the fuel may not be perfectly homogeneous. Therefore, local lacks of oxygen causes the combustion to be incomplete.

flue gas (Figure 2.3). Once separated, diverse CO_2 concentrations are presented in the literature spanning a range from 80%vol to 98%vol [8, 9, 13, 14]. The rest of the composition of the flue gas comprises excess of O_2, N_2, ash, other traces present in the air and some NO_x and/or SO_x. The nitrogen and the traces come from air ingress and the purity of oxygen below 100%vol.

As for post-combustion capture, a FGPU may be required to process the flue gas after the combustion so that the constraints of the combustion chamber and the CPU are met[3]. The flue gas is recirculated into the combustion chamber, before or after the FGPU (called wet or dry recycling, respectively) for two main reasons. First, the recirculation decreases the combustion temperature, which is considerably increased as a result of the combustion with O_2 [11, 15, 16]. Controlling the temperature is important to keep the same combustion chamber as that without capture. For this purpose, the quantity of recirculated flue gas is determined such that the oxygen reaches a concentration of 30%vol in the oxidizer [9, 13, 15, 16]. Second, as NO_x emissions are driven by the temperature, reducing the temperature by recirculating a portion of the flue gas lowers the formation of NO_x [14–16]. At the end of the process, 90% to 94% of CO_2 is recovered [17].

The key element of oxy-fuel combustion is the oxygen, produced most of the time via an ASU. Oxygen production by cryogenic distillation stands as the most common way to perform this task. Allam *et al.* [9] even emphasise that this is the only cost-effective technique, as large amounts of oxygen are required. In short, the air is first compressed, purified to get rid of the other constituents of the air, and finally cooled down to reach an oxygen stream with a concentration of roughly 95%vol. This system typically consumes 165 kWh/t_{O_2} to 240 kWh/t_{O_2} of electricity which leads to an increased energy penalty and costs, relative to the facility without capture [7, 9, 18]. Other techniques are emerging and are being developed as membrane separation. Oxygen can also be supplied from the oxygen produced as a co-product of the electrolysis. When using electrolysis as the source of oxygen, an ASU is still necessary as the production of oxygen via electrolysers will not always cover the oxygen demand to continuously capture the CO_2. Moreover, if the hydrogen comes from importations, oxygen production with an ASU becomes more competitive.

[3]Corrosion limits, concentration requirements for the CPU and for the combustion chamber are typical constraints.

Table 2.1: Summary of the advantages and drawbacks of the three capture strategies.

CO_2 capture strategies	Advantages	Drawbacks
Pre-combustion capture	- Production of H_2 - Increased CO_2 concentration	- High energy requirements - High capital and operating costs - Not easy for retrofitting
Post-combustion capture	- Easy for retrofitting - More mature	- Low CO_2 concentration begetting a high energy penalty and costs
Oxy-fuel combustion capture	- Very high CO_2 concentration - Low NO_x emissions - Appropriate for retrofitting	- High energy penalty and costs from the ASU

2.1.2 State of the art: CO_2 separation technologies

Several CO_2 separation technologies exist; including absorption, adsorption, membrane, cryogenic distillation, etc. Other techniques, particularly adapted to specific sectors such as CaO-looping, or still in research and development such as microalgae capture, are not covered in this review. To reach high separation efficiencies, the technology needs to be chosen appropriately depending on the application because these techniques depend on the characteristics of the flue gas and of the process [8]. These gas separators, integrated in the capture technologies described before, are summarised below.

Absorption

CO_2 separation by absorption can be either chemical or physical. The physical absorption is based on Henry's law. CO_2 is absorbed at high pressure and then the solvent or sorbent is regenerated with heat, pressure reduction or both [9, 19]. The chemical absorption is based on a chemical reaction between the CO_2 and the absorbent.

In both cases, the flue gas first enters the absorber from the bottom and the CO_2 enters in contact with the CO_2 lean absorbent. Then, the CO_2-rich absorbent is sent to a stripper where the absorbent is regenerated and the CO_2 is liberated. CO_2 is finally compressed for further utilisation or storage and the absorbent is pumped back to the absorber [12, 19] which finishes

the cycle. This cycle consumes a significant amount of energy to pump the flows and for the process in the absorber and the stripper [9].

Chemical absorption with post-combustion capture is widely agreed to be the most mature technology in the literature [7–9, 19] and among the multiple solvents and sorbents developed, the monoethanolamine (MEA) solvent is commonly used [8]. Another advantage of this solvent is the high CO_2 concentration achieved — up to 99%vol [9, 19].

However, solvent degradation caused by the high temperature and pressure, by the presence of O_2 and the remaining gas impurities is a disadvantage of this method. The efficiency is limited by the high energy requirement to regenerate the absorbent [8, 12]. Another issue is the CO_2 emissions begotten by the ammonia synthesis required for the manufacture of the solvent.

Adsorption

The principle of adsorption is described as molecules creating bonds with other molecules at the surface of a material. This concept is used to isolate CO_2 from other gases. Most of the systems are composed of two or three adsorption chambers, each filled with solid adsorbent, allowing the process to run continuously. When one chamber is adsorbing the CO_2, the second one is liberating the captured CO_2 and the last one is being regenerated[4] [8].

The adsorbent is fed by the flue gas at high pressure and low temperature to enhance the adsorption. The regeneration is then achieved by increasing the temperature or by decreasing the pressure, called temperature swing adsorption and pressure swing adsorption, respectively [9, 12].

The advantage of adsorption compared to absorption is that the regeneration is less energy-intensive [20, 21]. However, one of the main disadvantages of the adsorption capture is the low selectivity entailing that the CO_2 concentration needs to be high. Finally, the low capture capacity makes adsorption not suitable for high mass flow rate of flue gas [8, 12].

Membranes

The separation of CO_2 with a membrane is driven by the difference of partial pressure. Therefore, membrane separation is more effective when the feed has a high CO_2 concentration. This technique is currently used for natural gas sweetening [9], but a lot of researches show

[4] In the case of two chambers, when the first one is saturated, the flow of flue gas is deviated to the second one. While the second one is adsorbing, the first chamber desorbs the captured CO_2 and is regenerated until the second is saturated and the cycle goes on.

interest to make available new membranes due to the potential low environmental impact, high efficiency and lower complexity compared to the other separation techniques [8, 22].

Nonetheless, there are still gaps to be filled to make this method more attractive. First, the membrane is limited to strict thermal constraints as the temperature of the flue gas is limited to 100°C [8]. Second, more selective membranes need to be developed to avoid a large number of stages and to get a high-concentrated CO_2 stream especially if the flue gas has a low CO_2 concentration [8, 9, 12]. As for absorption, corrosion can damage the membranes begetting the need for a flue gas pretreatment [8].

Cryogenic separation

Cryogenic separation is a gas separation technique based on the condensation and sublimation properties of the gases [8]. For CO_2 separation, the flue gas is cooled down to temperature between -100°C and -135°C which is below the sublimation temperature of the CO_2. The CO_2 can then be separated from the other gases [7] by distillation or other approaches [8].

The main limitation of this method is the risk of water still present in the flue gas after being processed which can create obstruction by ice blocks in the systems. Additional units are then necessary to remove all the water [8, 22]. Another disadvantage is the high energy requirement leading to high costs. For this reason, flue gas with a high CO_2 concentration is preferable [12].

Cryogenic separation can achieve a CO_2 purity and recovery up to 99% according to Songa *et al.* [8]. Moreover, no solvent or sorbent is required — unlike for absorption and adsorption.

2.1.3 Choice of the CO_2 capture system for the port of Antwerp

In the previous section, it has been shown that the efficiency and the attractiveness of the CO_2 capture and separation technologies depend on the characteristics of the flue gas and of the target products. Hence, each plant in the port of Antwerp requires a specific CO_2 capture system to reach optimum efficiency. However, selecting a system for each plants in the port of Antwerp would be complex and is beyond the scope of this thesis. Therefore, among the technologies detailed in Sections 2.1.1 and 2.1.2, one suitable CO_2 capture system, considering the context of this study, will be chosen.

Kuramochi *et al.*[17] conducted a study comparing the different CO_2 capture strategies for each of the three following sectors: the cement sector, the iron and steel sector and for the refineries and petrochemicals. Based on an extensive literature review, several economic and technical parameters were standardised to make an apples-to-apples comparison. In summary,

Table 2.2: Summary of the advantages and drawbacks of the CO_2 separation technologies.

CO_2 separation technologies	Advantages	Drawbacks
Absorption	- High efficiency - Mature technology	- Absorbent degradation - High energy requirement for regeneration - Sensitive to corrosion
Adsorption	- Lower energy requirement than absorption	- Low selectivity - Low adsorption capacity
Membrane	- Low environmental impact - High efficiency - Low complexity	- Low selectivity - Sensitive to corrosion - Strict temperature limitations
Cryogenic separation	- CO_2 purity (up to 99%) - CO_2 recovery (up to 99%) - No need for solvent or sorbent	- Large energy requirement - High costs

they concluded that for the cement sector, post-combustion with a MEA solvent is the most economically attractive in the short-to-medium term, whereas CaO-looping is proved to be even more cost-effective in the long term. Concerning the iron and steel sector, CO_2 capture systems specific for this sector are compared, but none clearly stood out as all have different advantages and drawbacks. For the refining and petrochemical sector, oxy-fuel combustion was claimed to be more economically viable no matter the period of time because the CO_2 avoided cost[5] varies around 50–60 €/t_{CO_2} compared to more than 70 €/t_{CO_2} for the post-combustion.

As the port of Antwerp is composed of 12 chemical plants, whose 3 refineries and 10 power plants fueled with gas, oxy-fuel combustion could be a suitable capture technology in this case.

A second study realised a comparative assessment of the different CO_2 capture technologies [11]. This time, Kheirinik *et al.* [11] simulated the three capture technologies with a 230 MW coal power plant. They concluded that the total investments for pre-combustion are significantly higher than the other technologies. Oxy-fuel combustion appears to require the lowest total investments, but has the highest costs per ton of captured CO_2. Finally, considering the maturity and the lower impacts of retrofitting with post-combustion capture, they pointed out that this approach is the most suitable for an existing plant.

[5]The CO_2 avoided cost is defined as the carbon price so that the product cost is equal for either a plant without capture or the same plant with capture.

However, they considered that oxygen is fully produced by an ASU whereas in this specific case of the port of Antwerp, oxygen is available as a co-product of the electrolysis producing the hydrogen required for the methanation. Using oxygen from the electrolysers reduced the energy requirement of the ASU and thus lowers the energy costs [23]. The main disadvantage of oxy-fuel combustion is then reduced as the energy penalty is decreased. Using the electrolysers as the only source of oxygen is though not possible. As said in Section 2.1.1, if not enough O_2 is locally produced to meet the demand of the combustion, an ASU is still required to keep on supplying the combustion chamber.

Considering the advantages and drawbacks of the different techniques summarised in table 2.1 and 2.2 and the findings emphasised in this section, oxy-fuel combustion with oxygen produced from electrolysers and from an ASU seems to be the most suited CO_2 capture system for capturing CO_2 in the port of Antwerp when generalising for all its industries.

Though, this technique becomes less competitive in two cases. First, as the electrolysers consume a significant amount of electricity, some hydrogen may be imported from countries endowed with renewable energy in abundance. This means that the co-produced oxygen must be also transported over long distances. Therefore, the advantage of consuming less energy for the ASU by using the oxygen from the electrolysers is offset by the transport of the oxygen. Second, if utilising all the captured CO_2 is too energy-intensive, part of the CO_2 can be stored permanently, decreasing the quantity of hydrogen required for the methanation. Consequently, less oxygen will be produced by the electrolysers whereas the continuous CO_2 capture needs to be guaranteed. The production of oxygen by the ASU will then turn to be more important which raises the energy penalty implied by the oxy-fuel combustion capture. In these cases, post-combustion with chemical absorption by the monoethanolamine (MEA) solvent also stands as a good candidate due to its maturity and to its easy retrofitting of existing plants, despite the high energy intensity of the separation.

In conclusion, oxy-fuel combustion and post-combustion capture with the MEA solvent will be the two CO_2 capture technologies which will be used for the CO_2 capture in this study. The two next sections aim to outline their technical characteristics required for the study. The values are chosen based on the previous literature review. Finally, the method followed to quantify the mass flow rates and the energy flows is also presented.

Technical characteristics of oxy-fuel combustion capture

For the sake of simplicity, it is considered that the same fuel is burnt in all the combustion chambers of the industries of the port. The aggregated data of the European Pollutant Release and

Transfer Register (E-PRTR) database and the Global Infrastructure emission Database (GID)[6] points out that 22 industries[7] are catalogued in the port, whose 10 are reported as power plants fueled with natural gas. The others are chemical facilities, where at least 3 are refineries [24–27]. As stressed by Concawe ("The oil companies' European association for Environment, Health and Safety in refining and distribution") [28], natural gas progressively replaces oil for the combustion in refineries as a result of pollutant regulations. Therefore, most of the units of the port are fueled with natural gas and thus, it has been chosen as fuel. Specifically, the type of natural gas is high-calorific because Fluxys has announced that by 2024 no low-calorific gas will be distributed anymore[8] [29]. The average composition of the natural gas measured by Fluxys in the pipelines is shown in Table 2.3.

Table 2.3: Average properties of the high-calorific natural gas (H-gas) supplied in Belgium [29].

Properties	H-gas
Composition	
Methane (CH_4)	92.49%mol
Ethane (C_2H_6)	4.54%mol
Propane (C_3H_8)	0.79%mol
Butane (C_4H_{10})	0.29%mol
Pentane (C_5H_{12})	0.05%mol
Hexane[a] (C_6H_{14})	0.04%mol
Nitrogen (N_2)	0.89%mol
Carbon dioxide (CO_2)	0.9%mol
Helium (He)	0.01%mol
Others	
Molar mass	17.44 g/mol
LHV[b]	47 871 kJ/kg

[a] And superior hydrocarbons.

[b] Abbreviation: Lower Heating Value (LHV)

The parameterisation of the oxy-fuel combustion capture will now be detailed step by step following the flow diagram below (Figure 2.4).

[6] More details about these databases in Section 2.5.

[7] It should be noted that most of these industries comprise multiple processing units.

[8] Hereinafter, high-calorific natural gas will be referred to as natural gas.

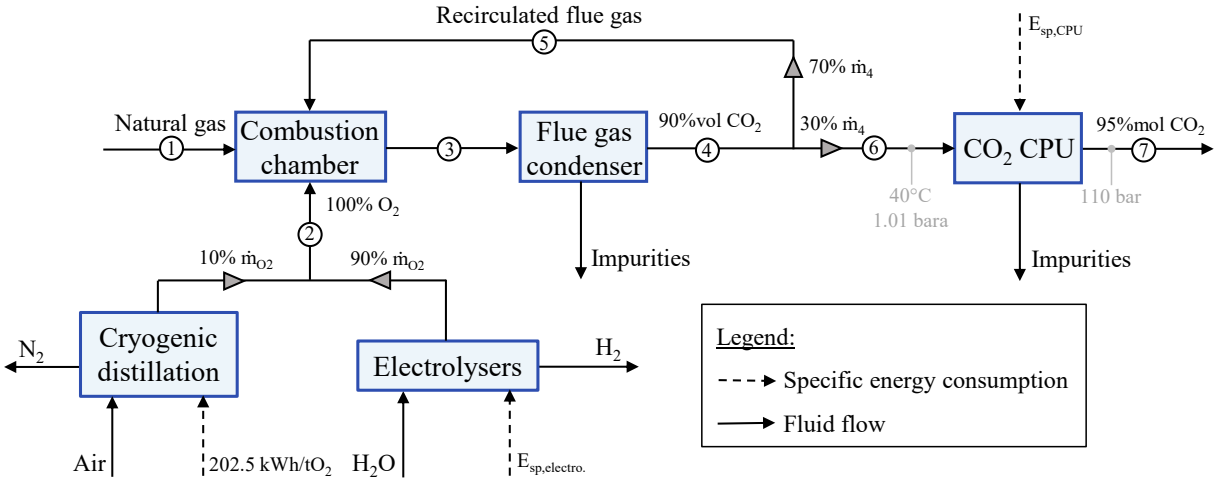

Figure 2.4: Parameterisation of oxy-fuel combustion capture. Abbreviation: compression and processing unit (CPU).

The ASU is a cryogenic distillation unit which produces oxygen and nitrogen, usually with a concentration of 95%vol and 5%vol, respectively [13, 15, 18]. However, pure O_2 has been considered to simplify the combustion equation (Eq. 2.5). It is assumed that 10% of the O_2 is produced by the ASU, while the rest comes from the electrolysers. Its nominal specific energy consumption is set to 202.5 kWh/t_{O_2}.

The Flue Gas Processing Unit (FGPU) is only constituted of a flue gas condenser, where it is assumed that all the water content is removed. In fact, no electrostatic precipitator to remove the ash and no flue gas desulphurisation system are assumed necessary, as no ash and no sulfur are produced in the combustion of natural gas. Additionally, the NO_x is already significantly reduced by the flue gas recirculation, as explained previously, so no $DeNO_x$ unit is included.

After the FGPU, 70% of the CO_2-rich gas (90%vol of CO_2) is recirculated to the combustion chamber, while 30% is directed to the CO_2 CPU [13]. This latter purifies the CO_2-rich stream from 90%vol to 95%mol concentration of CO_2 to be conformed with the CO_2 pipelines standard, ISO 27913 [30]. Additionally, this unit compresses the CO_2 to 110 bar with a multi-stage compressor [17, 31].

The number of stages (N) of this compressor is obtained by Eq. 2.3.

$$\frac{p_7}{p_6} = k^N \Leftrightarrow N = \log_k\left(\frac{p_7}{p_6}\right) \tag{2.3}$$

where p_7 and p_6, respectively, are the outlet (110 bar) and inlet pressures (1.01 bara). The compression ratio (k) is set to 3, under the recommendation of Ul Haq *et al.* [32] stating that a

compression ratio below 3.5 entails lower costs for a centrifugal CO_2 compressor.

The specific energy consumption of the compressor is derived by neglecting the energy consumption related to the purification and by assuming an adiabatic reversible compression (Eq. 2.4)[9]:

$$E_{\text{sp,CPU}} = \frac{Z_{CO_2} R T_6}{M_{\text{m,CO}_2\text{-rich}} \eta_{\text{is}} \eta_{\text{mec}}} \frac{N\gamma}{(\gamma - 1)} \left(\left(\frac{p_7}{p_6} \right)^{(\gamma-1)/N\gamma} - 1 \right) \tag{2.4}$$

where Z_{CO_2} is the CO_2 compressibility factor to take into account the non-ideal behavior of the CO_2 at 40°C and 1.01 bara (0.99553), R is the ideal gas constant (8.314 J/(mol K)), T_6 is the temperature at the inlet (40°C), $M_{\text{m,CO}_2\text{-rich}}$ is the molar mass of the CO_2-rich stream (computed with the molar composition of this stream), η_{is} is the isentropic efficiency (80%), η_{mec} is the mechanical efficiency (98%) and γ is the ratio of specific heats (c_p/c_v)(1.28) [17, 33]. The specific heat at constant pressure (c_p) and constant volume (c_v) are found under the assumption of a perfect gas at 40°C.

The molar mass of the flue gas with a 90%vol CO_2 concentration ($M_{\text{m,CO}_2\text{-rich}}$) after the water condensation is computed using its molar composition resulting from the combustion written as follows by taking into account all the above-mentioned assumptions[10]:

$$\begin{gathered} x_{f,\text{C}_z\text{H}_y}\,\text{C}_z\text{H}_y \;+\; x_{\text{f,N}_2}\,\text{N}_2 \;+\; x_{\text{f,He}}\,\text{He} \;+\; x_{\text{f,CO}_2}\,\text{CO}_2 \;+\; x_{\text{oxi,O}_2}\,\text{O}_2 \;+\; RFG \\ \rightarrow \\ \left(x_{\text{f,C}_z\text{H}_y} z + x_{\text{f,CO}_2}\right)\text{CO}_2 \;+\; x_{\text{f,He}}\,\text{He} \;+\; x_{\text{f,N}_2}\,\text{N}_2 \;+\; x_{\text{O}_2}\,\text{O}_2 \;+\; RFG \\ \text{with } RFG \;=\; \left(1 - x_{\text{oxi, O}_2}\right)\left(0.9\,\text{CO}_2 \;+\; 0.1\left(x_{\text{f,N}_2}\,\text{N}_2 \;+\; x_{\text{f,He}}\,\text{He} + x_{\text{O}_2}\,\text{O}_2\right)\right) \end{gathered} \tag{2.5}$$

where RFG stands for recirculated flue gas. The notation x refers to the molar fraction, the subscript f stands for fuel, the subscripts z and y are the equivalent number of C and H in the natural gas, respectively, and x_{O_2} is obtained by balancing the stoichiometric coefficients. $x_{\text{oxi,O}_2}$ is the composition of oxygen in the oxidizer set at 30%vol.

As the emissions target of the port is to cut down half of the emissions, the mass flow rate of pure CO_2 captured is known. Hence, the mass flow rate of the stream after compression is

[9] The numbered subscripts, such as 7 or 6, refer to the different states of the oxy-fuel combustion capture illustrated in Figure 2.3

[10] It should be noted that the gases are considered ideal. Hence, molar and volume concentration are equivalent.

also known by using the CO_2 concentration requirement in the pipelines:

$$\dot{m}_7 = \frac{\dot{m}_{\text{Antw},CO_2}/2}{\frac{0.95\, M_{\text{m},CO_2}}{M_{\text{m},7}}} \approx \frac{\dot{m}_{\text{Antw},CO_2}/2}{0.95} \quad \text{as } M_{\text{m},CO_2} \approx M_{\text{m},7} \tag{2.6}$$

where $\dot{m}_{\text{Antw},CO_2}$ is the annual CO_2 emissions in the port of Antwerp and where 95%mol is the mole fraction of CO_2 in the compressed stream. Though, it is considered that these two molar masses are close, so the formula is simplified.

The oxygen mass flow rate to obtain a composition of 30%vol is computed as:

$$\frac{\dot{m}_{O_2}/M_{\text{m},O_2}}{\dot{m}_{O_2}/M_{\text{m},O_2} + \dot{m}_5/M_{\text{m},CO_2\text{-rich}}} = x_{\text{oxi},O_2} \Leftrightarrow \dot{m}_{O_2} = \frac{x_{\text{oxi},O_2} M_{\text{m},O_2} \dot{m}_5}{\left(1 - x_{\text{oxi},O_2}\right) M_{\text{m},CO_2\text{-rich}}} \tag{2.7}$$

In the previous equation, $\dot{m}_5$, the mass flow rate of the recirculated flue gas (point 5 is represented in Figure 2.4) is still unknown. This latter is derived from $\dot{m}_7$ and by considering that during the purification, some CO_2 is released together with the impurities. Therefore, the capture rate is adjusted by a recovery efficiency (η_{rec}) of the CO_2 defined to 94% [17].

$$\dot{m}_5 = \frac{\dot{m}_7 0.7}{\eta_{\text{rec}}(1 - 0.7)} \tag{2.8}$$

where 0.7 corresponds to the 70% of recirculated flue gas.

It should be noted that the specific energy consumption of pumps, auxiliaries, etc. has not been taken into account in this study. The lifetime (40 years), investment and maintenance costs (2610.46 $€_{2015}/kg_{CO_2}$ and 64.8 $€_{2015}/kg_{CO_2}$, respectively) are all taken from Limpens's thesis [34].

Technical characteristics of the post-combustion capture

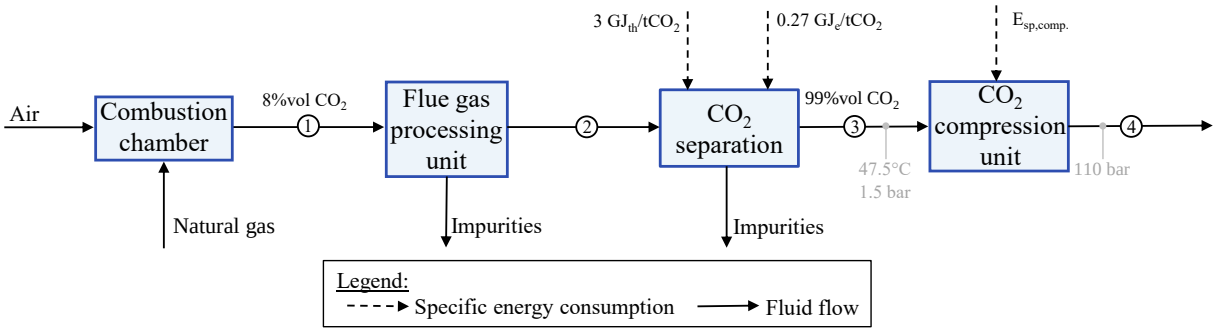

Figure 2.5: Parameterisation of post-combustion capture. Abbreviation: compression (comp.).

The assumptions for the fuel of the combustion are obviously the same as the previous section (Section 2.1.3). Following the flow diagram (Figure 2.5), natural gas feeds thus the combustion chamber producing a flue gas whose the CO_2 concentration is estimated between 7%vol and 14%vol (dry basis) in power plants and 8%vol (dry basis) in refineries and petrochemical plants [9]. The port of Antwerp being a petrochemical cluster, the CO_2 concentration is set at 8%vol. Before the separation of the CO_2, the flue gas is processed in the FGPU to comply with the thermal and quality constraints of the MEA solvent. For this reason, the flue gas is cooled down to 47.5°C by a direct contact cooler which eliminates the water content [12] and a $DeNO_x$ unit (e.g. selective non-catalytic reduction unit) reduces the NO_x concentration.

The absorption of the CO_2 with the MEA solvent consumes 3 GJ_{th}/t_{CO_2} of heat for the regeneration and 0.27 GJ_e/t_{CO_2} of electricity [9]. As said previously, the flue gas leaves the absorber with a 99%vol concentration [9, 20]. Hence, no additional purification is required to meet the quality standards of the gas network [30]. Still, the CO_2-rich gas is compressed from 1.5 bara to 110 bar [9]. The specific energy consumption of the compression is derived using Eq. 2.4. In this case, Z equals to 0.99839, the temperature at the inlet is 47.5°C, the specific heat ratio is 1.28 and the molar mass of the CO_2-rich stream is estimated as the one of CO_2 as the stream is almost CO_2 pure. For the rest, the same assumptions have been made.

As for oxy-fuel combustion capture, not all the CO_2 is captured in the process inducing a recovery efficiency of 87.5% [9]. Moreover, the specific energy consumption of the pumps, auxiliaries, etc. have also been neglected.

The mass flow rate of captured CO_2 at 99%vol concentration is defined following the same logic as that of oxy-fuel combustion capture. Half of the CO_2 emissions of the port are taken as input and are divided by the CO_2 concentration to get the mass flow rate of the CO_2-rich stream. Again, the molar mass at 99%vol is considered equal to the CO_2 molar mass.

$$\dot{m}_4 = \frac{\dot{m}_{\mathrm{Antw,CO_2}}/2}{\frac{0.99\,M_{\mathrm{m,CO_2}}}{M_{\mathrm{m,4}}}} \approx \frac{\dot{m}_{\mathrm{Antw,CO_2}}/2}{0.99} \quad \text{as } M_{\mathrm{m,CO_2}} \approx M_{\mathrm{m,4}} \tag{2.9}$$

The quantity of flue gas treated is significantly higher due to the low CO_2 concentration in the flue gas after the combustion. This mass flow rate is derived with the following equation:

$$\dot{m}_1 = \frac{\dot{m}_{\mathrm{Antw,CO_2}}/2}{0.08\eta_{\mathrm{reco}}} \tag{2.10}$$

where 0.08 corresponds to the CO_2 concentration in the refineries and petrochemical plants.

Finally, the same lifetime and cost parameters (investment and maintenance) as oxy-fuel combustion capture are taken: 40 years, 2610.46 $€_{2015}/kg_{CO_2}$ and 64.8 $€_{2015}/kg_{CO_2}$, respectively [34].

2.2 Water electrolysis

Hydrogen can be produced using different resources (coal, natural gas, renewable energy, etc.). In 2021, 96% of the hydrogen production was based on fossil fuels [35]. Only 4% correspond to water electrolysis. Water electrolysis is an endothermic reaction which splits the H_2O molecule into hydrogen and oxygen using electricity (Eq. 2.11).

$$2H_2O \rightarrow 2H_2 + O_2 \tag{2.11}$$

Three electrolysers exist to perform this reaction: the Solid Oxide Electrolyser (SOE), the Proton Exchange Membrane, also called Polymer Electrolyte Membrane Electrolyser (PEME) and the Alkaline Electrolyser (AE) [36]. These technologies can be classified into two categories: high-temperature electrolysis (SOE) and low-temperature electrolysis (PEME and AE). The next section aims to describe the main characteristics of these electrolysers (Table 2.4).

2.2.1 Elecrolysers fundamentals

Solid oxide electrolyser

Solid oxide electrolysers were developed in the 1980s, but a remarkable interest has only recently grown due to technological advances, the urge of climate change, calling for net zero emissions and the rise of the renewable energy shares in the energy mix which necessitates absorbing excess electricity [37]. During high-temperature electrolysis, steam flows at the cathode where H_2 and oxide ions are produced (Eq. 2.12). The reduced oxygen then goes through the membrane to the anode where it releases again electrons (Eq. 2.13).

$$\textbf{Cathode:} \quad H_2O + 2e^- \rightarrow H_2 + O^{-2} \tag{2.12}$$

$$\textbf{Anode:} \quad O^{2-} \rightarrow \frac{1}{2}O_2 + 2e^- \tag{2.13}$$

This process can be reversed [36, 38] and this cell has also the advantage of being adapted for the co-electrolysis of steam and CO_2 for the production of syngas [36, 37]. Moreover, operation between 700°C and 900°C improves the thermodynamic and kinetic conditions compared with low-temperature electrolysis which leads to a cell efficiency close to 100% [36, 39]. Despite

these advantages, SOE is still only at the research stage [36, 39]. Moreover, important materials limitations still need to be overcome for a durable operation and high-grade heat is required [36, 37, 39].

Alkaline electrolyser

In contrast with the SOE, alkaline electrolysis has been used at a commercial scale since the beginning of the 20th century [36, 40]. AE stands as the most used electrolyser globally [41]. This technology consists of two electrodes (a cathode and an anode) immersed in an alkaline electrolyte, separated by a membrane. At the cathode, liquid water is broken down into hydrogen and hydroxide anions (Eq. 2.14). The hydrogen is then collected while the hydroxide anions flow through the membrane, driven by the electric field, to the anode where they are oxidised in oxygen (Eq. 2.15).

$$\textbf{Cathode:} \quad 2H_2O + 2e^- \rightarrow 2OH^- + H_2 \tag{2.14}$$

$$\textbf{Anode:} \quad 2OH^- \rightarrow \frac{1}{2}O_2 + H_2O + 2e^- \tag{2.15}$$

Despite offering the advantage of being mature, its efficiency is lower than the two other electrolysers. Its start-up time is also higher than the PEME, making it less suitable to be supplied by renewable energy. Another limitation is that the AE is bulkier than the PEME as the electrolyte is liquid in contrast to the solid electrolyte of the PEME [36, 39].

Proton exchange membrane electrolyser

The PEME is made of a solid electrolyte through which protons circulate, hence the name proton exchange membrane or polymer electrolyte membrane. These protons are produced at the anode fed by liquid water, where the following reactions occur:

$$\textbf{Cathode:} \quad 2H^+ + 2e^- \rightarrow H_2 \tag{2.16}$$

$$\textbf{Anode:} \quad H_2O \rightarrow \frac{1}{2}O_2 + 2H^+ + 2e^- \tag{2.17}$$

Several advantages make this technology particularly suited for coping with the intermittency of renewable energy compared to the alkaline one. In fact, the operation is assured up to the full load range and it has a lower start-up time than both the AE and the SOE [36, 39]. The design conception also sustains higher pressure and the solid electrolyte leads to a more compact system compared to the liquid electrolyte of the AE [39, 40]. On the other side, less PEMEs are developed at a commercial scale [41] and the development of a membrane with specific properties, withstanding high pressure, increases the costs [40].

Table 2.4: Summary of the advantages and drawbacks of the three water electrolysis technologies.

Electrolysers	Advantages	Drawbacks
Solid oxide electrolyser	- High efficiency - Reversible and co-electrolysis ability	- Research stage - Material challenges
Alkaline electrolyser	- Mature	- Low flexibility - Low operating pressure
Proton exchange membrane electrolyser	- Low start-up time - Compact - Flexible operation	- Expensive membrane development

2.2.2 Choice of the electrolyser for this study

Now that the different types of electrolysers have been reviewed, the technology suited for this case study is going to be defined. It has been pointed out that SOE is still not mature enough compared to AE and PEME. Additionally, high-grade heat is necessary, unlike these ones. Concerning these last two, it has been underlined that PEME has a higher efficiency. As the flexibility of the electrolysers is a key element of PtG, to be able to operate intermittently, PEME is preferred in this research.

Technical characteristics of the proton exchange membrane electrolyser

In this section, as it has been done for the chosen capture systems (Section 2.1.3), the main technical characteristics of the PEME are going to be determined. It should be noted that nominal values are computed as the mean of the values' range.

Buttler *et al.* [36] have conducted a market survey of the water electrolysis systems to compare the technologies based on their actual performances and characteristics. It came out from their review that the specific energy consumption of the PEME system is 5.75 kWh/Nm^3. The system does not include only the stack, but also auxiliaries such as pumps, water treatment, etc.[11]. Water requirement can not be neglected. Using the stoichiometric coefficients of the water electrolysis reaction (Eq. 2.11), 9 kg_{H_2O} is consumed by each kg of hydrogen. Though the electrolyser manufacturer Cummins [42] specified a water use between 13 kg_{H_2O}/kg_{H_2} and 17 kg_{H_2O}/kg_{H_2} due to the losses. The nominal value is then set to 15 kg_{H_2O}/kg_{H_2}. Water availability

[11] The external compression is not included.

can be problematic in some regions, especially with climate change increasing the frequency and intensity of drought. However, special attention is given to avoid this problem in the port of Antwerp [43] and seawater can supply the electrolyser after desalination.

Unlike SOE, low-temperature electrolysis such as PEME does not use heat as energy input. Due to higher losses in the cell, the voltage applied is greater than the thermoneutral voltage[12]. As a result, while part of the generated heat supplies the endothermic reaction, coolers are needed to maintain the cell at constant temperature (50–80°C) [36]. The rest of this heat is recovered and can be transported to the district heating network (DHN). Burrin *et al.* [44] analysed the quantity of heat produced by a PEME and the economical impact of supplying it to local networks. In their paper, they have found out that an electrolyser system of 1 MW operating 5 hours per day produces 312 kW_{th} of extracted heat and 18.7 kg_{H_2}/h which corresponds to 16.68 kWh_{th}/kg_{H_2}.

The other initial parameters are outlined in Table 2.5.

Table 2.5: Summary of the parameters of the proton exchange membrane electrolyser system.

Parameters	Symbol	Value	Ref.
Requirements			
Specific energy consumption	E_{sp}	5.75 kWh/Nm^3	[36]
Specific water use	$E_{sp,w}$	15 kg_{H_2O}/kg_{H_2}	[42]
Economic parameters			
Investment cost	c_{inv}	800 $€_{2015}$/kW	[45–47]
Operation cost	c_{maint}	3.5% of c_{inv}	[36, 45]
Others			
Heat production	q	16.68 kWh_{th}/kg_{H_2}	[44]
Efficiency (LHV)	η	53%	[36]
Lifetime	*lifetime*	20 y	[36, 48]
Capacity factor	$c_{p,expected}$	90%	[34]

2.3 CO_2 methanation

Methane can be produced by the combination of CO_2 and H_2. This reaction, known as the Sabatier reaction, can be either biological or catalytic. Biological methanation is operated at low temperatures (below 70°C), with microbes playing the role of catalysts [45, 49]. This process,

[12] The thermoneutral voltage is the voltage to be applied in a cell to avoid heat integration.

still under development, is not considered in this work. The CO_2 methanation[13] is an exothermic reaction, favoured at temperatures around 300°C, whose the stoichiometry is shown in Eq. 2.18:

$$\textbf{CO}_2\textbf{ methanation:} \quad CO_2 + 4H_2 \rightarrow CH_4 + 2H_2O \quad \Delta H_{298} = -165 \text{ kJ/mol} \qquad (2.18)$$

Methanation is commonly proceeded in fixed-bed reactors, but other systems such as microreactors are gaining interest [49, 50]. The catalytic reactors are cooled to maintain the reactors to optimal temperature conditions and the heat recovered can be recycled for other applications. Beyond the researches around reactors, catalysts are the key element of the methanation. Nickel is a widely used catalyst due to its low price and high activity. Although it has been demonstrated that ruthenium is the most active metal, its high price limits its utilisation in large-scale applications [49, 51].

It is worth noting that the methane produced is not 100% pure. In fact, the CH_4 concentration after the steps of the reactions reaches approximately 80% (mass basis) as unreacted CO_2 and H_2 also compose the raw-SNG [52, 53]. A small portion of water and impurities present in the reactants are also contained in the CH_4-rich gas. An additional step of raw-SNG upgrading is then needed to comply with the quality requirement of the gas network.

2.3.1 Technical characteristics of the methanation unit

The heat released by the hydrogenation of CO_2 can be either used at high temperatures to meet the heat demand of the post-combustion capture, or to feed the low-temperature District Heating Network (DHN). As no heat consumption has been considered for the oxy-fuel combustion capture, the second option is preferred to be able to compare the two capture technologies with the same assumptions. The heat quantification is based on the paper of Chauvy *et al.* [31]. They investigated the environmental and techno-economic performances of an integrated PtG system in a cement plant. The modelling of this unit resulted in 0.17 $GJ_{th}/GJ_{raw\text{-}SNG}$ which is converted to 2.26 kWh_{th}/kg_{SNG} by assuming the same mass energy density for raw-SNG and SNG.

Either the amount of CO_2 or H_2 determines the quantity of SNG produced based on the stoichiometric coefficients of Equation 2.18 and adjusted by the efficiency of the reaction set to 77% [45]. The average properties of the natural gas flowing in the Belgian pipelines listed in Table 2.3 are taken as the ones of the SNG after the upgrading step.

The lifetime, the capacity factor estimated *a priori*, the efficiency and the economic pa-

[13] CO_2 methanation will be hereinafter referred to as methanation.

rameters of the methanation unit for 2030 are reported in Table 2.6.

Table 2.6: Summary of the parameters of the methanation unit.

Parameters	Symbol	Value	Ref.
Economic parameters			
Investment cost	c_{inv}	333.4 €$_{2015}$/kW	[46]
Operation cost	c_{maint}	3% of c_{inv}	[54]
Others			
Heat production	q	2.26 kWh$_{th}$/kg$_{SNG}$	[31]
Efficiency (LHV)	η	77%	[45]
Lifetime	*lifetime*	25 y	[45, 54]
Capacity factor	$c_{p,expected}$	86%	[34]

2.4 CO_2 storage

CO_2 storage techniques have been mastered for decades now with the first projects of enhanced oil recovery developed in the 1960s [55]. Nevertheless, the Convention for the Protection of the Marine Environment of the North-East Atlantic (OSPAR Convention) limits the transboundary transport and the disposal of pollutants in the marine environment. In 2007, this Convention has been modified paving the way for carbon storage projects in Europe [56]. Henceforth, the number of CCS projects is mushrooming and this chapter first aims to present a quick overview of CO_2 storage and then, the possibilities of CO_2 storage for the port of Antwerp.

2.4.1 Fundamentals of CO_2 storage

Once compressed, the CO_2 can be transported by different means, namely, pipelines, ships, roads and railway tankers. On the one side, ships and trucks can take flexible transport routes, but require intermediate storage for loading and unloading to avoid traffic bottlenecks. Underground and tank storage are the two existing intermediate storage approaches. On the other side, pipelines transport continuously the CO_2 to the platform making intermediate storage unnecessary. As said in Section 2.1, the pressure in pipes is of the order of around 100 bar and the pressure drop occurring in the pipes is offset by sub-compression stations [7]. CO_2 purity is also carefully controlled to avoid any damage or pipe degradation [7, 57]. Onshore, pipelines are acknowledged as the most attractive method as it offers large-capacity transportation over greater distances, unlike trucks and train carriers that have a limited capacity. Offshore, ships

and pipelines are both viable methods, although both have advantages and drawbacks. A combination of pipeline networks together with ships is often the chosen option for current projects [7, 57].

Geological storage allows the permanent storage of CO_2. Saline aquifers, depleted oil, and gas fields, unmineable coal beds, and the deep ocean have the potential to perform this task. Deep ocean storage is based on the fact that at high depth (more than 3 km), the density of the CO_2 becomes greater than the surrounding flows leading the CO_2 to sink. This technique is rather controversial due to environmental concerns. CO_2 storage in unmineable coal beds goes along with enhanced methane recovery. Similarly to enhanced oil recovery, the CO_2 is injected underground to recover trapped methane in the coal seams. In Europe, saline aquifers and depleted oil and gas fields constitute most of the storage capacity [58]. Bolscher *et al.* [59] have estimated a total theoretical potential of 300 Gt for CO_2 storage which is in line with the estimation of Vangkilde-Pedersen [58] underlining a capacity of 360 Gt. Nonetheless, they pointed out a practical estimation of 117 Gt [58]. In Belgium, 1 Gt has been claimed to be the conservative storage potential [60]. To put things in perspective, the E-PRTR reported that 24.4 Gt_{CO_2} have been emitted in 2020 by large industries[14] in Europe [24]. Consequently, the storage capacity is big enough to sequestrate CO_2 over a few decades. Despite the room for onshore CO_2 storage, public acceptance constrained most of the projects to be realised offshore [59].

2.4.2 Opportunities for the port of Antwerp

Mainly under the supervision of Fluxys, a CO_2 transport network, connecting the main industrial clusters of Belgium with these of neighbouring countries, is planned to be built. Antwerp, Zeebrugge and Ghent have been naturally selected to welcome CO_2 terminal infrastructures for offshore sequestration [61]. In Antwerp, the ambitions are big as they aim to build one of the "first and largest multimodal open access CO_2 export facilities in the world" [62].

Antwerp is linked with three main CCS projects: Northern Lights [63], CO_2TransPorts [64] and of course, Antwerp@C [6]. Northern Lights is a cross-border project connecting capture clusters across 7 European countries. First, CO_2 is transported by ship to a Norwegian terminal for intermediate storage and then, by pipeline for sequestration in saline aquifers in the North Sea. The first stage of development is expected to be complete by 2024 with a target of 1.5 Mt_{CO_2} stored each year and then, they consider expanding the capacity up to 5 Mt_{CO_2} depending on the market demand [63]. CO_2TransPorts' objective is to develop the essential infrastructure for efficiently capturing, transporting and storing CO_2 across the port of Antwerp, Rotterdam and

[14] Large industries are defined as industries emitting more than 0.1 Mt_{CO_2}/yr.

the North Sea Port [64]. Other projects developed in France or the Netherlands can benefit the port of Antwerp through future collaborations (Aramis, Dartagnan, etc.).

Table 2.7: Summary of the parameters of the geological CO_2 storage.

Parameters	Symbol	Value	Ref.
Economic parameters			
Investment cost	c_{inv}	24.9 $€_{2015}/t_{CO_2}$	[65]
Operation cost	c_{maint}	55.3 $€_{2015}/t_{CO_2}$	[65]
Other			
Lifetime	*lifetime*	40 y	[65]

The costs of CO_2 transport and permanent storage vary significantly across the studies due to the lack of developed projects and the storage strategy. This latter involves choices about the mode of transport, pipe geometry, characteristics of the storage (location, storage depth, capacity, type of storage facility, and so on), etc. Depending on the project, the costs then highly fluctuate. Although, an estimation of the economic parameters of geological storage is required for this study. For this purpose, the work of Oei *et al.* [65] has been used. They defined a model minimising the costs of a strategy to deal with the CO_2 emissions (by either buying CO_2 allowances or storing CO_2). The CO_2 sources, the storage location, the storage capacity and the carbon price are then accounted in the model. In the case of offshore storage only, with a carbon price of 100 $€/t_{CO_2}$ and on a period of 40 years, they found out the economic parameters reported in Table 2.7.

Table 2.8: Summary of the parameters of the tank CO_2 storage. Abbreviation: storage (sto.)

Parameters	Symbol	Value	Ref.
Economic parameters			
Investment cost	c_{inv}	65.1 $€_{2015}/kg_{CO_2}$	[34, 66]
Operation cost	c_{maint}	1% of c_{inv}	[66]
Sto. characteristics[a]			
Input sto. efficiency	$\eta_{sto,in}$	100%	[34]
Output sto. efficiency	$\eta_{sto,out}$	100%	[34]
Self-discharge	$\%_{sto_{loss}}$	0 $\frac{\%}{h}$	[34]
Other			
Lifetime	*lifetime*	30 y	[34]

[a] CO_2 storage is considered perfect.

In the Antwerp@C project, short-term CO_2 storage will also be needed in the case of CO_2 utilisation. While CO_2 will be captured continuously, hydrogen availability depends on imports

and domestic production. Temporary CO_2 storage is then necessary to buffer variations of hydrogen supplies. For these reasons, steel tank storage has been selected for onshore intermediate storage and its characteristics are listed in Table 2.8.

2.5 Estimation of the CO_2 emissions

Two databases have been used to get an estimation of the CO_2 emissions in the port of Antwerp: the European Pollutant Release and Transfer Register (E-PRTR) [24] and the Global Infrastructure Emission Database (GID) [25–27]. These two databases report plant-level data covering different sectors. Some data was missing in both datasets, so they have been aggregated to create one complete database. In the following sections, these two databases will first be presented, and then an explanation of the resulting database will be provided.

2.5.1 European Pollutant Release and Transfer Register

Under the Industrial Emissions Directive, the E-PRTR regulation has been established to foster transparency, to make available comparable and trustworthy data and to facilitate the monitoring of the pollutant releases of the industries [67]. It encompasses industries of each European Union member state, as well as Iceland, Liechtenstein, Norway, Serbia, Switzerland and the United Kingdom, emitting more than 0.1 Mt/y of pollutants in the air or water. The database contains the specific sector[15] of the facility, the geographic coordinates, the type of pollutant and the value of the emissions. Data is available from 2007 to 2022 [24]. The pollutant release quantification is either achieved by measurements, computation or estimation. The method chosen by the operator of each facility can then impact the consistency and the quality of the data. Therefore, guidance documents have been released to enhance accuracy and consistency in the emissions quantification.

2.5.2 Global Infrastructure Emission Database

The GID was created by Tsinghua University in China in 2020. Their goal is to provide reliable data to support research and policy decisions. They provide data of 231 countries of the world for three sectors: power plants, cement and iron and steel sector. This facility-level database includes detailed information about the facility, the location and the CO_2 emissions[16] for the year 2019. However, part of this information (e.g. geological coordinates) is only avail-

[15] The different sectors included in this regulation are listed in Appendix A.
[16] The emissions are estimated based on computations.

able on request to the GID team. I contacted them, but I was informed that additional data can not be shared, as they are working on papers [25–27].

2.5.3 Aggregated database

Surprisingly, some data is missing in the E-PRTR database. For example, the recent emissions of a significant steel industry such as Thy-Marcinelle in Charleroi are not available. As a result, some units are included in the E-PRTR dataset and not in the GID and vice versa. Moreover, additional data, such as the distinction between process and fuel emissions for the cement industry or the type of fuel used for the power plants is available in the GID, whereas the geological coordinates are only included in the E-PRTR database. Hence, to ensure that the input data is more complete, the two databases of 2019 have been thoroughly merged in order to complete the missing data and to keep the common data. This step is not straightforward as the provided information by the two databases is different. Comparing the two databases based on the geological coordinates, for instance, could have been simple, but this information is not available for the GID. Therefore, after a manual cleaning of spelling mistakes or poorly categorised industries, the databases have been compared based on the city name where possible and manually otherwise. Finally, missing geological coordinates have been added using Google information. In the end, a complete database resulting of the aggregation of those two databases has been created including industries of the Netherlands and Belgium. Major differences in CO_2 emissions value between common facilities can be noted. As the E-PRTR database is an official and controlled database, the values of this latter are initially used and then, if not available, the emissions of the GID are taken.

2.6 Projection of hydrogen availability

The second essential input of PtG technologies is hydrogen. An estimation of the hydrogen availability in 2030 will be presented in this section.

In the *Plan national pour la reprise et la résilience*, Belgium planned to reach an electrolyser capacity of 150 MW by 2026 through incentives and policies. The determination of the 2030 target is in the pipeline within the government [68]. To contextualise, the EU has the ambition to install a capacity of 40 GW producing 10 Mt_{H_2} by 2030 [68] which involves the need for an increased electrolyser manufacturing capacity and production of renewable electricity supplying these electrolysers. By assuming an expected capacity factor of 90%, the quantity of hydrogen expected to be produced domestically can be computed.

On the other hand, Belgium has a limited capacity of renewable electricity production. The country will thus need to import hydrogen to satisfy the demand. In this context, the report on the vision and strategy for hydrogen stated that Belgium will import 20 TWh in 2030 and 200–350 TWh in 2050 of hydrogen molecules and hydrogen derivatives to meet its demand, and acts as a transit hub for its bordering countries. The imported hydrogen will transit by the North Sea, by pipelines connecting the South of Europe with North Africa and by ships. Its importing price is set to 125.4 $€_{2015}$/MWh.

Further, it is outlined that 30% to 60% of the available hydrogen by 2050 will be used directly for the demand of hydrogen molecules and the remaining 40% to 70% will be used for the production of e-fuels [69]. Even if these last numbers are projections for 2050, they are the only values found in the literature, so I have assumed the same ratio for 2030. Moreover, the share of demand for hydrogen for the methanation is assumed as the same for e-fuels. Hence, the total quantity of available hydrogen for the production of methane is estimated as 55% of both the imported hydrogen and of the hydrogen domestically produced.

2.7 Energy system modelling with EnergyScope Typical Days

The energy system is modelled with EnergyScope Typical Days (ESTD). ESTD is an open-source energy model funded via collaboration between UCLouvain and EPFL (a Swiss university). The version used is the regional version which is focused on one region (Belgium in this case) and the *snapshot* one which optimises the energy system for one target year (2030 in this study).

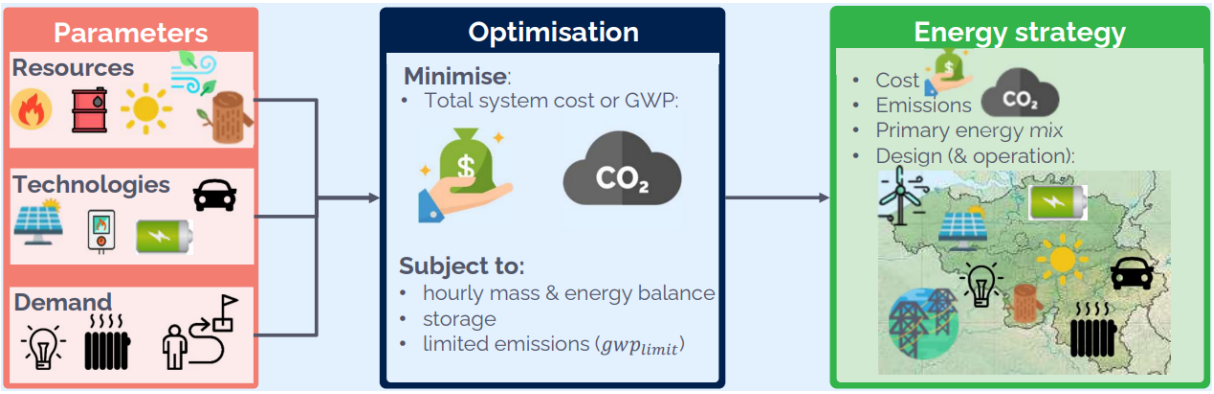

Figure 2.6: Overview of the EnergyScope Typical Days model.

Conceptually, the energy system is composed of demands divided into four categories (heat, electricity, mobility and non-energy demand) that need to be satisfied. Resources are avail-

able such as wind, gas, electricity, etc. and are converted by energy conversion technologies to meet these demands (e.g. wind turbines). The model optimises then the operation of these technologies to minimise either the total cost or the total greenhouse gas emissions of the system.

Mathematically, given parameters characterising the technologies and the resources (costs, lifetime, availability, etc.), the model linearly optimises the variables (e.g. the installed capacity of wind turbines) to minimise either the total cost or the Global Warming Potential (GWP) limit of the system so that all constraints are satisfied (Figure 2.6). The optimisation is performed with an hourly resolution. To avoid an endless computational time, the yearly time series are clustered in 12 typical days representing a whole typical year.

All the resources and types of demands are represented as *layers*. *Layers* are defined by Gauthier Limpens, one of the founders of ESTD as: "all the elements in the system that need to be balanced in each time period" [34]. The layers are linked to each other by the technologies which convert the energy of one or several layer(s) into one or multiple layers. An illustration of the concept of layers is shown in Figure 2.7. The hydropower plant uses the energy of rivers to produce electricity. Both the rivers and the electricity are layers linked by the hydropower plant technology. The generated electricity can then satisfy part of the electricity demand. Though, the electricity can also supply heat pumps to produce heat. Similarly, the heat layer can supply the heat demand or be stored with thermal storage technologies. Technologies like cogeneration have more than one output and are thus linked with the corresponding layers. All of these interactions between energy carriers and technologies create a complex network. In ESTD, this network is defined by 28 resources, 101 technologies and 10 types of demands defining the energy system.

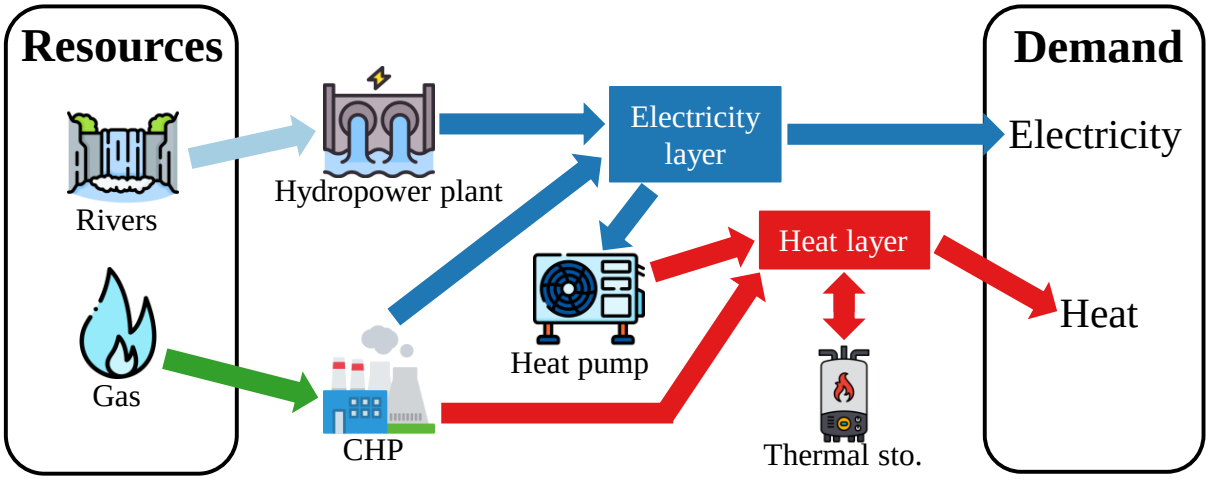

Figure 2.7: Illustrative example of an energy system modelled with EnergyScope Typical Days. Abbreviations: combined heat and power (CHP), storage (sto.). Figure inspired from [34].

In ESTD, the GHG emissions are computed based on the indirect emissions related to the resources. The indirect emissions of a resource account for its production, transport and combustion. The emissions related to the construction and the end-of-life of the conversion technologies are not accounted. This method of accounting follows the definition of the International Energy Agency [34]. It means that the captured CO_2 does not decrease the total GHG emissions of the system. Actually, the CO_2 available in the air or in the flue gas of industries is considered as a free resource (such as the wind) that capture technologies can consume to produce captured CO_2. The captured CO_2 can then be used or stored by other technologies.

2.7.1 Implementation

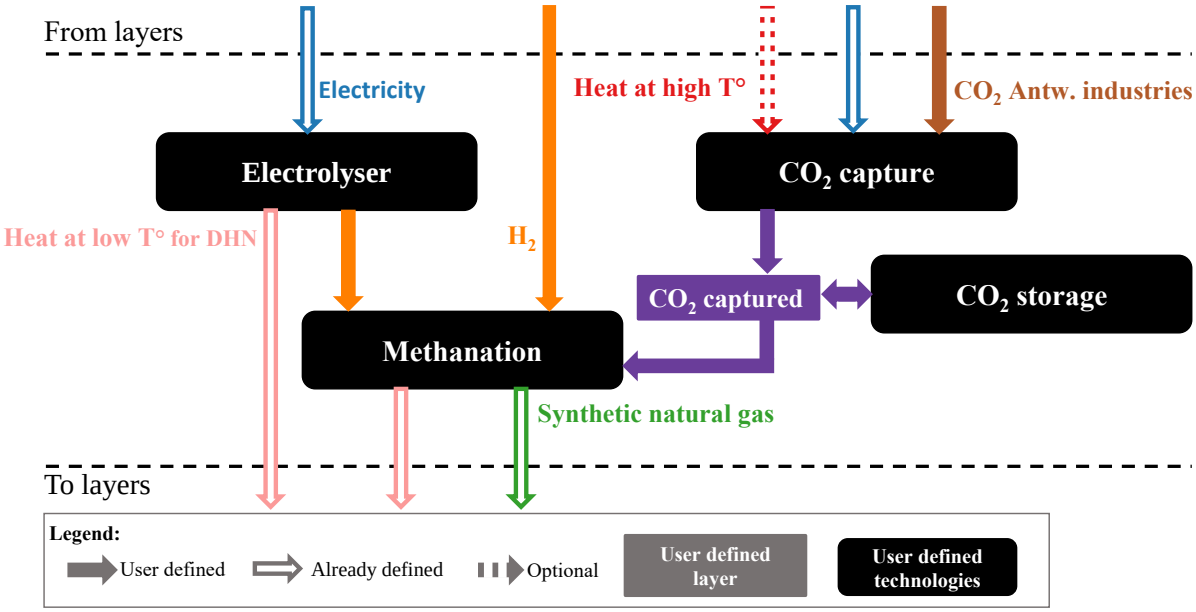

Figure 2.8: Overview of the implementation made on EnergyScope Typical Days. The optional arrow represents the case where post-combustion capture (heat supply required) or oxy-fuel combustion capture is implemented (no heat supply required). Abbreviations: district heating network (DHN), Antwerp (Antw.).

The described network of interactions between layers models the Belgian energy system. Within this system, a subsystem has been added. This subsystem characterises the decarbonisation plan of the port of Antwerp (Figure 2.8). It is composed of the following technologies: a post-combustion capture or oxy-fuel combustion capture technology (Section 2.1.3), a Proton Exchange Membrane Electrolyser (PEME) (Section 2.2.2), a methanation unit (Section 2.3.1) and a CO_2 storage technology (Section 2.4.2). The CO_2 storage technology is modelled in a way to allow either a temporary storage or a permanent storage. Following the same logic as the illustrative example of Figure 2.7, this subsystem has been implemented as follows. The CO_2

contained in the flue gas of the industries of the port of Antwerp is a free resource. It is captured with one of the two capture technologies. Both capture technologies consume electricity, and heat at high temperature is consumed additionally with post-combustion capture. The captured CO_2 forms then a layer that supplies the methanation and interacts with the CO_2 storage technology. On the other side, H_2 is produced by the PEME or imported, and consumed by the methanation. The availability of the imported hydrogen is set to 11 TWh which corresponds to 55% of the foreseen 20 TWh (Section 2.6). The way it is implemented creates thus a subsystem of interdependent technologies only interacting together. In this way, the captured CO_2 comes inevitably from the industries of the port and not from the air, for instance. In the same way that the hydrogen is consumed only by the methanation and not by trucks.

The tables and figures summarising the parameters of the capture technologies (Figures 2.4 and 2.5), the PEME (Table 2.5), the methanation unit (Table 2.6) and of the CO_2 storage (Table 2.8) characterise the conversion technologies of this subsystem.

Concerning other choices in the model, the total cost is optimised and the GWP limit is set as the GWP limit projected for 2030 (55,000 $kt_{CO_2,eq}/y$)[17]. Knowing that Belgium aims for a GHG emissions mitigation of 47% compared to 2005 and that the total GHG emissions amount to 126 $Mt_{CO_2,eq}$ in 2005 [70], this limit is rather ambitious. The CO_2 from the Antwerp industries is considered pure from the point of view of the model as the specific energy requirements are all expressed per kt of pure CO_2. The captured CO_2 has a CO_2 concentration of 99%vol and 95%mol for post-combustion capture and oxy-fuel combustion capture, respectively.

The compilation of this implementation in ESTD will provide the results on the energy system and the economy. These results will be compared with the original version of ESTD for 2030 and the same GWP limit, which will be called the reference case. To be clear, this implementation of ESTD does not depict a different scenario. They are actually the same scenarios for 2030, but with additional information concerning a project in the country.

2.8 Economic analysis

The economic viability and impacts of PtG on the energy system, modelled with ESTD, are assessed with two methods: the Levelised Cost of Energy (LCOE) and the breakdown of the total cost. The prices are all expressed in $€_{2015}$[18] and the values are the estimated prices for 2030.

[17] 55 $Mt_{CO_2,eq}/y$ is found by assuming a linear decrease of 15 $Mt_{CO_2,eq}/y$ from 100 $Mt_{CO_2,eq}/y$ in 2015.
[18] See Appendix C.1 for more details.

The production cost of SNG with PtG can be determined with the Levelised Cost of Synthetic Natural Gas (LCSNG). The production cost can be computed either *a posteriori* once the project is up and running with the exact values, or *a priori* to verify the profitability before investing in the facility. In this case, the LCSNG is calculated *a priori* with expected and estimated values. The LCSNG depends on the three main technologies composing the PtG system. Therefore, the LCOE of each technology is first computed using an adaptation of the formula proposed by Gauthier Limpens [34]:

$$crf(i) = \frac{i_{\text{rate}} \left(1 + i_{\text{rate}}\right)^{lifetime(i)}}{\left(1 + i_{\text{rate}}\right)^{lifetime\ (i)} - 1} \qquad \forall i \in PtG\ TECHS \quad (2.19)$$

$$LCOE_{\text{capex}}(i) = \frac{c_{\text{inv}}(i) \cdot crf(i)}{c_{\text{p,expected}}(i) \cdot 8760} \qquad \forall i \in PtG\ TECHS \quad (2.20)$$

$$LCOE_{\text{opex}}(i) = \sum_{res \in RES_i} c_{\text{op}}(res) \cdot f(i, res) - \sum_{prod \in SOLD\ PROD_i} c_{\text{op}} \cdot f(i, prod) + \frac{c_{\text{maint}}(i)}{c_{\text{p,expected}}(i) \cdot 8760}$$

$$\forall\, i \in PtG\ TECHS \quad (2.21)$$

where *PtG TECHS* represents the set of technologies constituting the PtG technology, *lifetime* is the lifetime of the technology and $c_{\text{p,expected}}$ is the expected capacity factor. The LCOE is obtained as the sum of CAPEX[19] related LCOE ($LCOE_{\text{capex}}$) and OPEX[20] related ($LCOE_{\text{opex}}$). The $LCOE_{\text{capex}}$ is found by the multiplication of the investment cost (c_{inv}) and the capital recovery factor (crf). The capital recovery factor is defined as the ratio of a constant annuity and the present value of this annuity with an interest rate (i_{rate}) over a certain number of years, here defined as the lifetime. The $LCOE_{\text{opex}}$ is computed as the sum of the maintenance cost (c_{maint}) and the specific cost of the resources (c_{op}) required for the operation. Additionally, the sale of some products (e.g. heat at low temperature) is taken into account. These products are part of the set named *SOLD PROD*. *f(i, res)* equals to the quantity of resource by unit of the main output of the technology. The same logic is applied for *f(i, prod)*[21]. Once the LCOE of each technology is computed, the LCSNG is obtained by the sum of the LCOE of each technology weighted by the quantity of the main output of the corresponding technology by unit of SNG[22].

[19] CAPEX stands for Capital Expenditure.
[20] OPEX stands for Operational Expenditure.
[21] The matrix with the f values are shown in Appendix B.
[22] More details about the development and the formulas are available in Appendix C.2.

The sold elements are the heat at low temperature for DHN (from the electrolysers and the methanation unit) and the captured CO_2. The nitrogen produced by the air separation unit with oxy-fuel combustion capture, the solvent consumption (roughly 1.6 $kg_{MEA}/t_{CO_2\ separated}$ [9]) in the absorber and the oxygen by-product are not accounted in the economic analysis. The price for heat at low temperature and high temperature is considered the same and equals to the one of the Netherlands [71] (77.66 $€_{2015}/MWh_{th}$). Pietzcker *et al.* [72] studied the impact of tighter emissions allowances of the European emissions trading system and found out that the carbon price will increase up to 129 $€/t_{CO_2}$ in this scenario. Knowing that the average carbon price in 2022 was 80.8 $€/t_{CO_2}$ [73] which is already above the projection made by the European Union in 2016 (around 20 $€/t_{CO_2}$ for 2022 [74]), 129 $€/t_{CO_2}$ seems to be a relevant estimation of the future carbon price. Then, the water requirement for the electrolysers has also been taken into account. As said in Section 2.2.2, water consumption amounts to 13–17 kg_{H_2O}/kg_{H_2} [42]. Water price for industries is unknown, so a wide range is found in the literature (0.69 $€_{2015}/m^3$ to 5.62 $€_{2015}/m^3$) [75, 76]. The mean of this range is assumed as the nominal value.

The lifetime, the capacity factor, the investment and maintenance costs of the technologies have been indicated in the sections dedicated to their technical parameterisation[23]. The other economic parameters are shown in Table 2.9.

Table 2.9: Economic parameters of the system.

Parameters	Value	Ref.
Carbon price (c_{carbon})	129 $€/t_{CO_2}$	[72]
Heat price[a]	77.66 $€_{2015}/MWh_{th}$	[71]
Water price	3.15 $€_{2015}/m^3$	[75, 76]
Electricity price (c_{elec})	145 $€/MWh_e$	[53]
Interest rate	1.5%	[34]

[a] Same price has been chosen for low-temperature heat and high-temperature heat.

The total cost is computed as the sum of the costs related to the technologies and the resources. The costs of the technologies are the result of the sum of their annualised investment cost ($crf\boldsymbol{C}_{\mathbf{inv}}$) and their operation and maintenance cost ($\boldsymbol{C}_{\mathbf{maint}}$). These two costs are calculated with similar equations, i.e. the installed capacity ($\boldsymbol{F}$) multiplied by their respective specific cost (c_{inv} and c_{maint}). The cost of the resources ($\boldsymbol{C}_{\mathbf{op}}$) is derived by summing over each hour of the typical days, the specific cost of the resource (c_{op}) multiplied by the operation on each of period

[23] See Figures 2.4 and 2.5 for the capture, Table 2.5 for the electrolyser and Table 2.6 for the methanation.

and by the duration of this period.

$$\boldsymbol{C}_{\mathbf{tot}} = \sum_{j \in TECH} \left(crf(j)\boldsymbol{C}_{\mathbf{inv}}(j) + \boldsymbol{C}_{\mathbf{maint}}(j) \right) + \sum_{i \in RES} \boldsymbol{C}_{\mathbf{op}}(i) \tag{2.22}$$

$$with\ crf(j) = \frac{i_{\text{rate}} \left(i_{\text{rate}} + 1 \right)^{lifetime(j)}}{\left(i_{\text{rate}} + 1 \right)^{lifetime(j)} - 1} \qquad \forall j \in TECH \tag{2.23}$$

$$\boldsymbol{C}_{\mathbf{inv}}(j) = c_{\text{inv}}(j)\boldsymbol{F}(j) \qquad \forall j \in TECH \tag{2.24}$$

$$\boldsymbol{C}_{\mathbf{maint}}(j) = c_{\text{maint}}(j)\boldsymbol{F}(j) \qquad \forall j \in TECH \tag{2.25}$$

$$\boldsymbol{C}_{\mathbf{op}}(i) = \sum_{t \in T | \{h,td\} \in T\_H\_TD(t)} c_{\text{op}}(i)\boldsymbol{F}_{\mathbf{t}}(i,h,td)t_{\text{op}}(h,td) \qquad \forall i \in RES \tag{2.26}$$

2.9 Sensitivity analysis

The process modelling, the economic analysis and the energy system analysis are sensitive to the uncertainty of parameters. Especially, the annual CO_2 emissions in the port of Antwerp, the projection of the hydrogen demand for the methanation and the quantity of oxygen produced by the ASU rather than by electrolysers are highly uncertain.

Table 2.10: Range of parameters values sensitive to uncertainty.

Parameters	Unit	Min.	Max.	Ref.
$c_{\text{inv,PEME}}$	€$_{2015}$/kW	300	1300	[45–47]
$c_{\text{maint,PEME}}$	% of c_{inv}	2	5	[36, 45]
$c_{\text{inv,metha}}$	€$_{2015}$/kW	293.6	373.2	[46]
$c_{\text{inv,}CO_2\text{tank sto.}}$	€$_{2015}$/kg$_{CO_2}$	34.4	95.8	[34, 66]
H_2 demand for metha.	%	40	70	[69]
$\dot{m}_{\text{Antw,}CO_2}$	Mt$_{CO_2}$/y	11.7	17	[5, 24]
c_{elec}	€/MWh$_e$	40	250	[53]
c_{carbon}	€/t$_{CO_2}$	80	129	[72]

Specifically for the economic analysis, the investment and maintenance costs are not certain as the maturing, the number of projects, the specific characteristics of each technology and even external factors impact the costs. Two scenarios have then been defined: a cheap one determined by taking the lower range of the costs and an expensive one determined by the upper limit. For the LCSNG, the impact of the volatility of the electricity price and the carbon price is evaluated.

The range of the uncertain parameters is shown in Table 2.10. The uncertainty of some pa-

rameters as the costs of the CO_2 capture or the operation cost of the methanation is not accounted due to the lack of information about these values for 2030.

Chapter 3

Results and discussion

3.1 Preliminary

3.1.1 Process modelling

The aggregated database reports that 14.34 Mt_{CO_2} were emitted by the industries in the port of Antwerp in 2019 which represent 15.9% of the total CO_2 emissions in Belgium [3]. As a reminder, the target is to halve the CO_2 emissions of the port by 2030. Hence, the emissions mitigation target is estimated to 7.17 Mt_{CO_2}. Knowing the CO_2 concentration after the CO_2 capture and the recovery efficiency, the mass flow rates in the CO_2 capture systems are then computed (Section 2.1.3). For the post-combustion capture, it means that 7.24 Mt/y of CO_2-rich stream are captured and that the mass flow rate of flue gas after the combustion is 102.4 Mt/y. For the oxy-fuel combustion capture, the mass flow rates are also derived. 7.55 Mt/y flow after the CO_2 CPU and 18.7 Mt/y are recirculated to the combustion chamber. The mass flow rate of oxygen to obtain an oxygen concentration of 30% in the oxidizer is 6 Mt/y.

The compression unit of the oxy-fuel and post-combustion capture is made up of 5 and 4 stages, and consumes 31.46 kWh/t_{CO_2} and 28.82 kWh/t_{CO_2}, respectively.

Post-combustion capture is significantly more energy-intensive than oxy-fuel combustion capture due to the large energy need for the CO_2 separation (Figure 3.1). The heat required for the regeneration of the MEA solvent is especially large as it multiplies by around 9 times the energy requirement of the post-combustion capture. Nonetheless, the decision of retrofitting an existing plant with oxy-fuel combustion capture is not straightforward. In fact, despite a lower energy need, this technology remains less mature and is more difficult to embed in an existing facility. Moreover, the ASU specific energy consumption is sensitive to the assumption of the percentage of oxygen produced by this unit rather than by the electrolysers, but this will be analysed in the sensitivity analysis (Section 3.4.1).

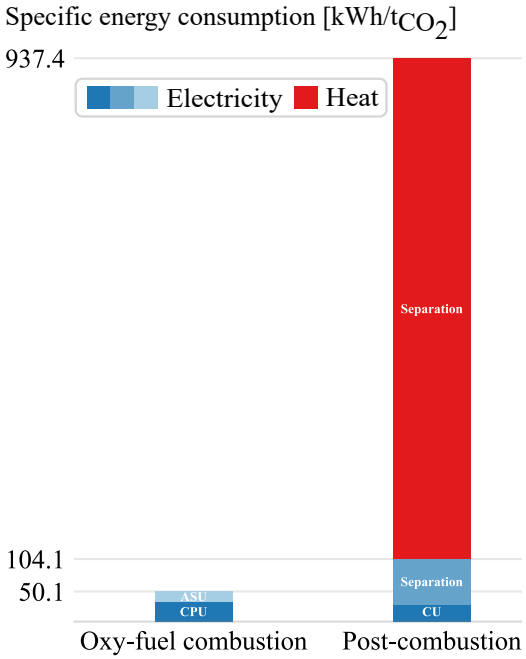

Figure 3.1: The breakdown of the specific energy consumption of the two capture technologies indicates how post-combustion capture is more energy-intensive than oxy-fuel combustion capture due to its heat requirement. Blue colours refer to electricity and red colour refers to heat. Abbreviations: air separation unit (ASU), compression and processing unit (CPU), compression unit (CU).

3.1.2 Economic analysis

The cost-effectiveness of PtG is assessed with the LCSNG obtained with the nominal values of Table 2.9. It results in a production cost of 371.8 €/MWh_{SNG} and 388.6 €/MWh_{SNG} for oxy-fuel and post-combustion capture, respectively (Figure 3.2). The OPEX related LCSNG of the electrolysers drives clearly the LCSNG due to their high electricity consumption, while the CAPEX related LCSNG contributes slightly to the LCSNG. A carbon price of 129 €/t_{CO_2}[1] entails a negative levelised operation cost of the CO_2 capture and even a negative levelised cost of captured CO_2. It means that at this carbon price, capturing CO_2 is profitable. Naturally, the operation cost of the oxy-fuel combustion capture is lower because no heat is needed for its operation unlike post-combustion capture. The drop between the hydrogen production costs and the PtG costs is explained by the heat produced via the methanation which is sold.

[1] As a reminder, the average carbon price in 2022 was 80.8 €/t_{CO_2} [73], whereas the European Commission projected a price of around 20 €/t_{CO_2} for the same year [74]. Therefore, 129€/t_{CO_2} seems realistic for 2030.

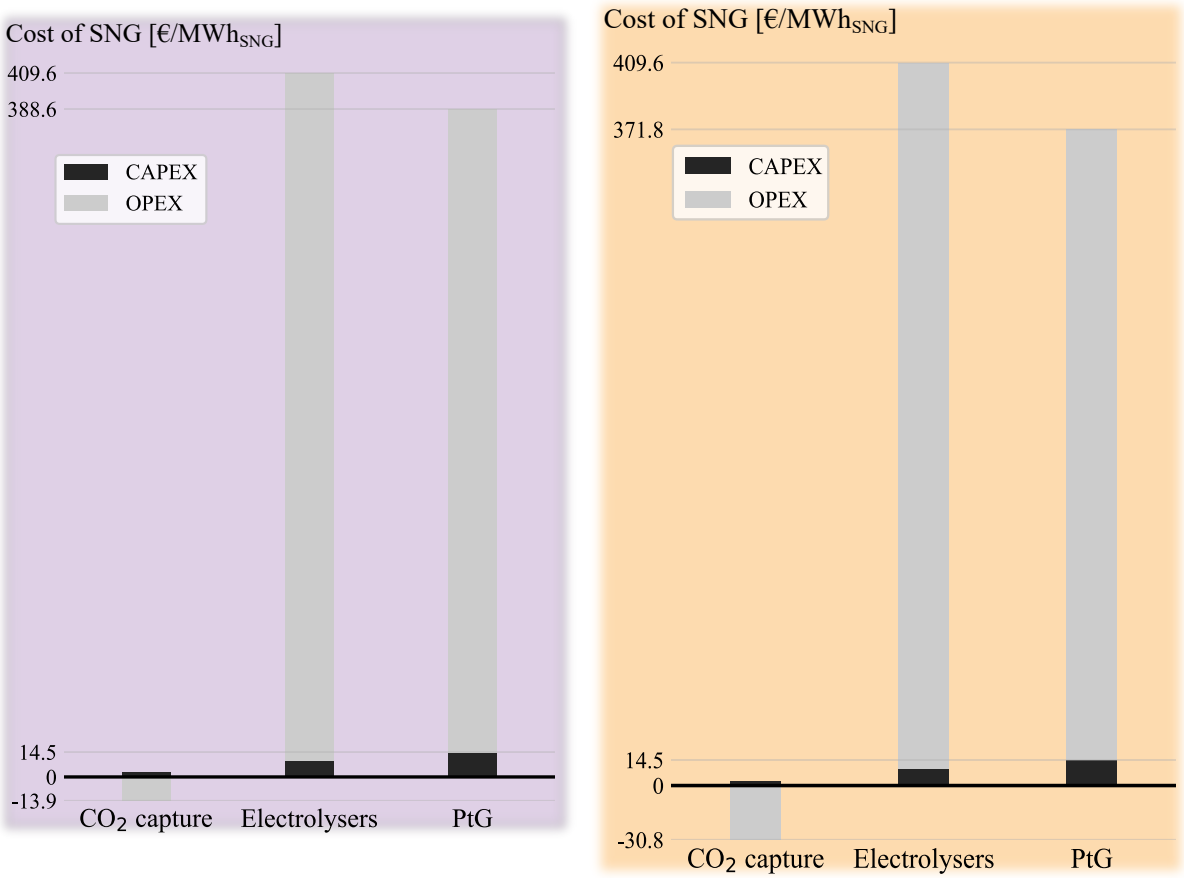

(a) Post-combustion capture.

(b) Oxy-fuel combustion capture.

Figure 3.2: The breakdown of the levelised cost of synthetic natural gas shows that the operational expenditure of the electrolysers is the main driver of the cost.

3.1.3 Energy system

For a GWP limit of 55 $Mt_{CO_2,eq}/y$, the optimisation of the energy system performed by ESTD results in no installation of the subsystem representing the PtG project in the port of Antwerp (described in Section 2.7.1). In this energy system model, the total GHG emissions do not account the captured CO_2 as it only accounts the emissions related to the resources usage. Hence, as long as the costs of PtG are greater than other ways of supplying gas, the model does not use this technology. However, it does not mean the GWP limit has no impact on the installed capacity. Actually, if this limit decreases, the share of renewable is expected to increase leading to an increasing need of coping with peaks of electricity production. The model may thus use the PtG system among other storage technologies to absorb these peaks. The impact of the costs and the GWP limit on its installed size is assessed in Section 3.4.1.

To be able to assess how the energy system is modified when the implemented subsystem is installed, an additional constraint in the model is required. Two scenarios are defined with this

additional constraint.

The first one represents the situation when all the captured CO_2 is used for the production of SNG. In other words, no CO_2 is stored underground. For this scenario, the constraint forces the amount of SNG produced by methanation, so that all the captured CO_2 is required for the reaction.

The second one characterises the situation when the quantity of SNG produced corresponds to the utilisation of the projection of available hydrogen for the methanation[2]. It is expected that this methanation reaction will only require the utilisation of a portion of the captured CO_2. Hence, part of the captured CO_2 will be stored underground. For this scenario, the corresponding quantity of produced SNG is constrained in a similar way to the previous scenario. In addition, half of the CO_2 emissions are still constrained to be captured, which will result in stored CO_2.

In the two following sections, the full utilisation and the partial utilisation of the captured CO_2 are going to be assessed and discussed in detail.

3.2 Full utilisation of the captured CO_2

3.2.1 Energy analysis

Focusing on oxy-fuel combustion capture with no H_2 import, using all the captured CO_2 corresponds to a production of 28.17 TWh_{SNG} (Figure 3.3). For this production, 88.8 TWh_e are consumed whose 99.6% supply the electrolysers. Therefore, the energy intensity of the CO_2 capture technology is relatively minor. This huge electricity consumption of the electrolysers is even comparable[3] to the final electricity consumption in 2021 [3]. On the other side, 23.76 TW_{th} is recovered for the DHN during the water electrolysis and the methanation process. The difference in energy production between the two capture technologies is explained by two reasons. On the one side, the mass flow rate of captured CO_2-rich stream is higher for the oxy-fuel combustion capture which implies a greater H_2 and SNG mass flow rate (Section 2.3.1). On the other side, post-combustion capture requires more electricity and heat per ton of CO_2. Overall, the combination of these two elements still results in a bigger energy production in the case of oxy-fuel combustion capture. When the expected H_2 importation by 2030 (11 TWh) is taken into account, the electricity consumption and the production of heat at low temperature

[2] The determination of the future hydrogen available for the methanation is described in Section 2.6.

[3] They are equal when rounded to one decimal and expressed in TWh, but it is not the case with no approximation.

obviously drop down. The optimisation performed by ESTD leads to the maximum import of hydrogen because importing hydrogen is cheaper than producing it with electrolysers[4] and because Belgium has a limited production capacity of renewable energy. The scenario illustrated with darker colours is the optimised one. Still, questions can arise concerning the potentiality of producing such a massive quantity of excess electricity by 2030. Moreover, the outcomes of ESTD indicate an installed capacity of the electrolysers equals to 10 GW. Developing such a massive electrolysers capacity by 2030 is rather unrealistic.

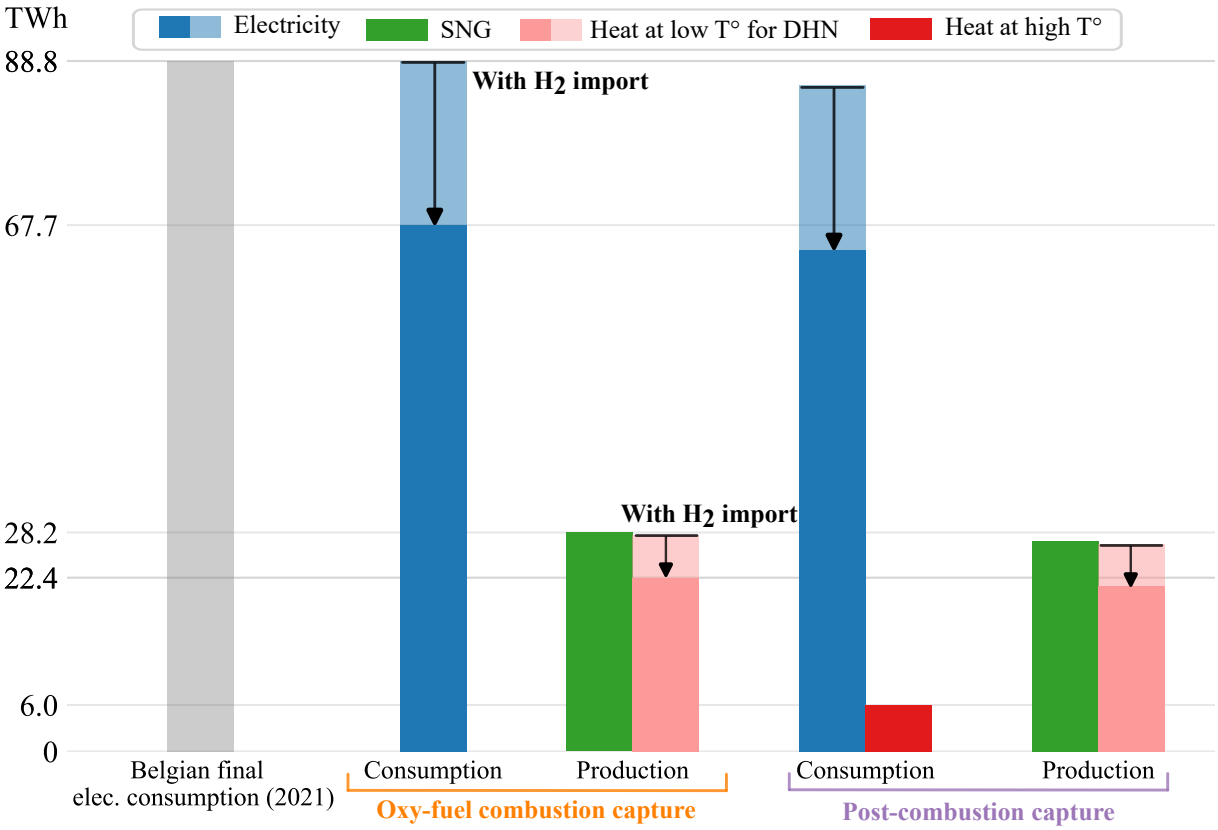

Figure 3.3: The energy production and consumption of a power-to-gas system supplied with all the captured CO_2 of the industries of the port of Antwerp show the massive electricity consumption by the electrolysers. Abbreviations: synthetic natural gas (SNG), district heating network (DHN), electricity (elec.).

An insight of the electricity mix resulting of this massive electricity need is illustrated in Figure 3.4.

Compared with the case with no implementation of CCU in the port of Antwerp, a great increase of the total electricity production is noticed, due to the energy requirement described previously. This is achieved by raising the photovoltaic (PV), the industrial gas Combined Heat

[4] In the model, the hydrogen import is, in fact, cheaper than producing domestically, even though this is uncertain.

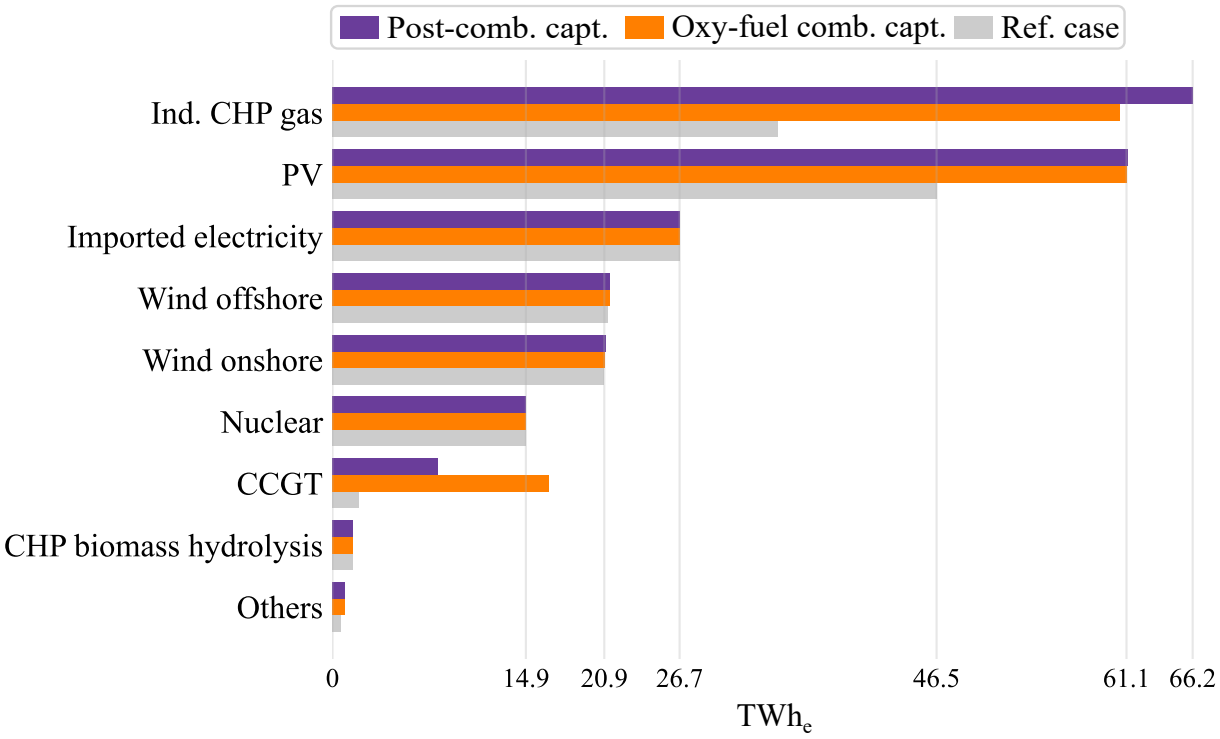

Figure 3.4: The comparison of the electrical mix with and without power-to-gas in the port of Antwerp illustrates how the important additional electricity requirement is produced, when all the captured CO_2 is used. Abbreviations: combustion (comb.), capture (capt.), industrial (ind.), combined heat and power (CHP), photovoltaic (PV), combined cycle gas turbine (CCGT).

and Power (CHP) and the Combined Cycle Gas Turbine (CCGT) production. A minor increase of the production by the offshore and onshore wind turbines and by the technologies included in the other category occurs too. This category gathers all the conversion technologies generating less than 1 TWh$_e$, i.e. the hydropower plants and the conversion of biomass to methanol. The slight rise is caused by the latter one. The reason is that the methanol production, whose by biomass, increases considerably compared to the reference case[5]. This additional electricity production is a straightforward result of the consumption of the PtG system. Though, the production also increases to compensate for the increased losses, proportional to the production.

Oxy-fuel combustion capture induces less electricity production by CHP than with post-combustion capture because this latter has a heat requirement which is supplied by CHP. This difference is partially offset by a greater production of the CCGTs for the oxy-fuel combustion capture.

The PV electricity production leads to an installation of the maximum capacity reachable, corresponding to 59.2 GW[6]. With an objective of 600 GW of installed capacity of PV by 2030

[5]Detailed information about this change is given at page 41.

[6]The maximum PV capacity of 59.2 GW is found by assuming that 250 km^2 of well-oriented roofs are available

in Europe [77], this estimation almost represents 10% of the European target for such a small and dense populated country as Belgium. The wind turbines installation also hits the upper limit for the three cases (10 GW for offshore and 6 GW for onshore wind turbines). Although, a little more electricity is generated over the year relative to the reference case. The imported electricity is also at the maximum of what can be imported. In the model, the nuclear capacity declines over the years to comply with the political decision of phasing-out of nuclear in Belgium. Starting from 5.9 GW in 2015, a capacity of 2 GW is still available in 2030. Hence, the nuclear electricity production in the three cases corresponds to this 2 GW.

Compared with the reference case, 69.6% more gas is consumed in the case of post-combustion capture. This additional gas, consumed by the CCGTs, the CHPs and the boilers, comes from methanation, but the gas import also raises from 105.14 TWh to 162.74 TWh (Figure 3.5). The other technologies consume the same amount of gas, just like the other production methods do for the production.

This large natural gas importation enhances the dependency of Belgium relative to the exporting countries. Moreover, whereas PtG takes place in a context of decarbonisation, one can conclude that it has the opposite effects based on these results. However, it should be kept in mind that ESTD does not account for the CO_2 emissions mitigation entailed by the CO_2 capture.

In the case with PtG, more imported gas is burnt which leads to an increase of the total GHG emissions. Though, the GWP limit is the same, so this increase occurs at the expense of the emissions related to another fossil fuel. In fact, the GHG emissions caused by the light fuel oil are curtailed. The production of High-Value Chemicals (HVC) by the light fuel oil is then substituted by the methanol. The methanol is produced from biomass (29%) and renewable methanol importation (71%). In summary, the light fuel oil is replaced by biomass and renewable methanol.

Similar conclusions are drawn with oxy-fuel combustion capture[7].

and that the total daily irradiation is 2820 Wh/m^2 with a capacity factor of 23% [34].

[7] The Sankey diagram of the gas flows for oxy-fuel combustion capture is shown in Appendix D.1.

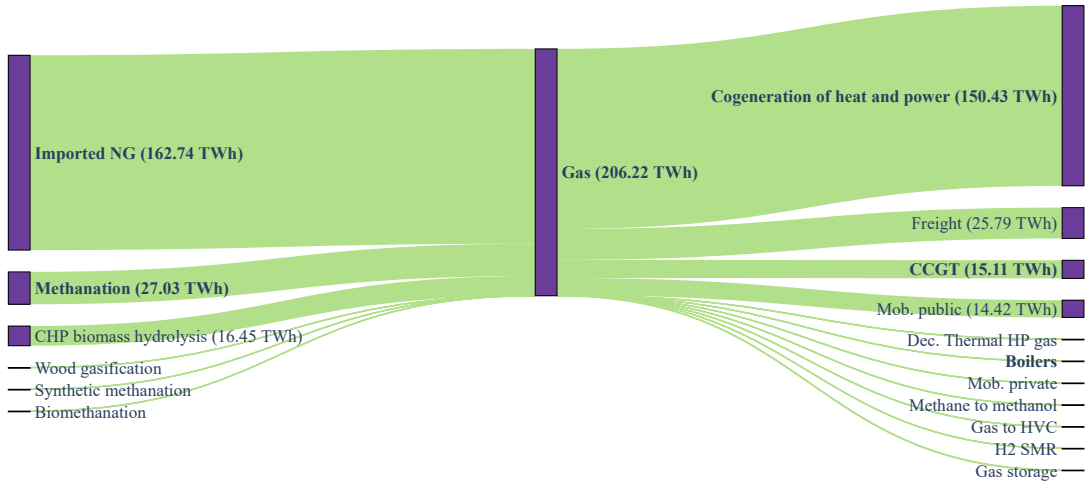

(a) Gas flows with power-to-gas in the port of Antwerp with post-combustion capture.

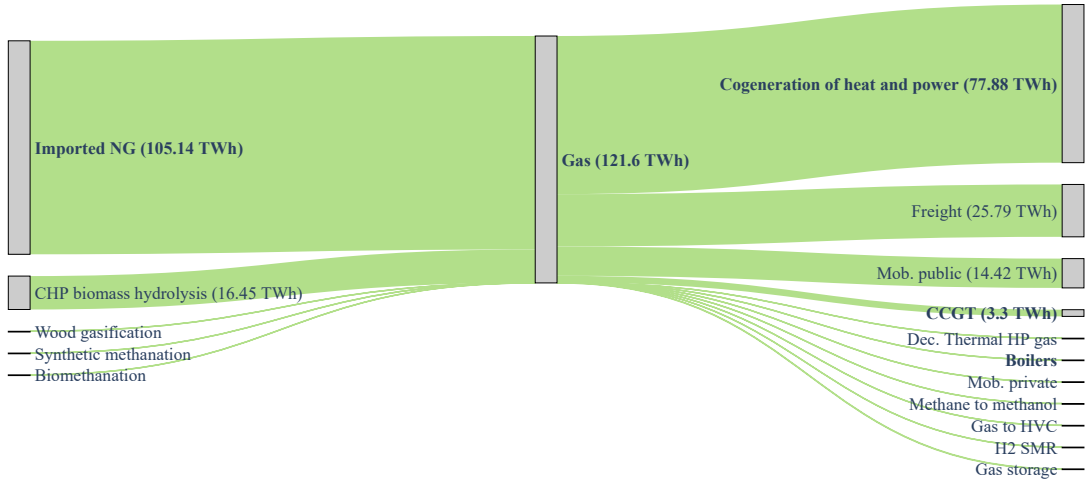

(b) Gas flows without power-to-gas in the port of Antwerp.

Figure 3.5: The comparison of the gas flows between case (a) and (b) indicates that despite producing gas by methanation, the imported natural gas is 1.5 times bigger with power-to-gas in the port of Antwerp. Names in bold emphasise the differences between the reference case and the case with the utilisation of the captured CO_2. Gas naming refers to either natural gas or synthetic natural gas. Abbreviations: imported (imp.), natural gas (NG), combined heat and power (CHP), combined cycle gas turbine (CCGT), decentralised (dec.), heat pump (HP), mobility (mob.), high-value chemicals (HVC), steam methane reforming (SMR).

3.2.2 Economic analysis

Those modifications in the energy system beget investments and additional costs. The difference of total cost amounts to 6.4 b€$_{2015}$/y (increase of 14.8%) and to 6.5 b€$_{2015}$/y (increase of 14.9%) for oxy-fuel and post-combustion capture, respectively. These annual additional costs represent 1.2% of the gross domestic product of Belgium in 2022. To put it in perspective, the record-breaking floods of 2021 entailed total expenses of 2.5 b€, according to the report of Assuralia [78]. Therefore, the additional costs implied by the production of SNG with half of

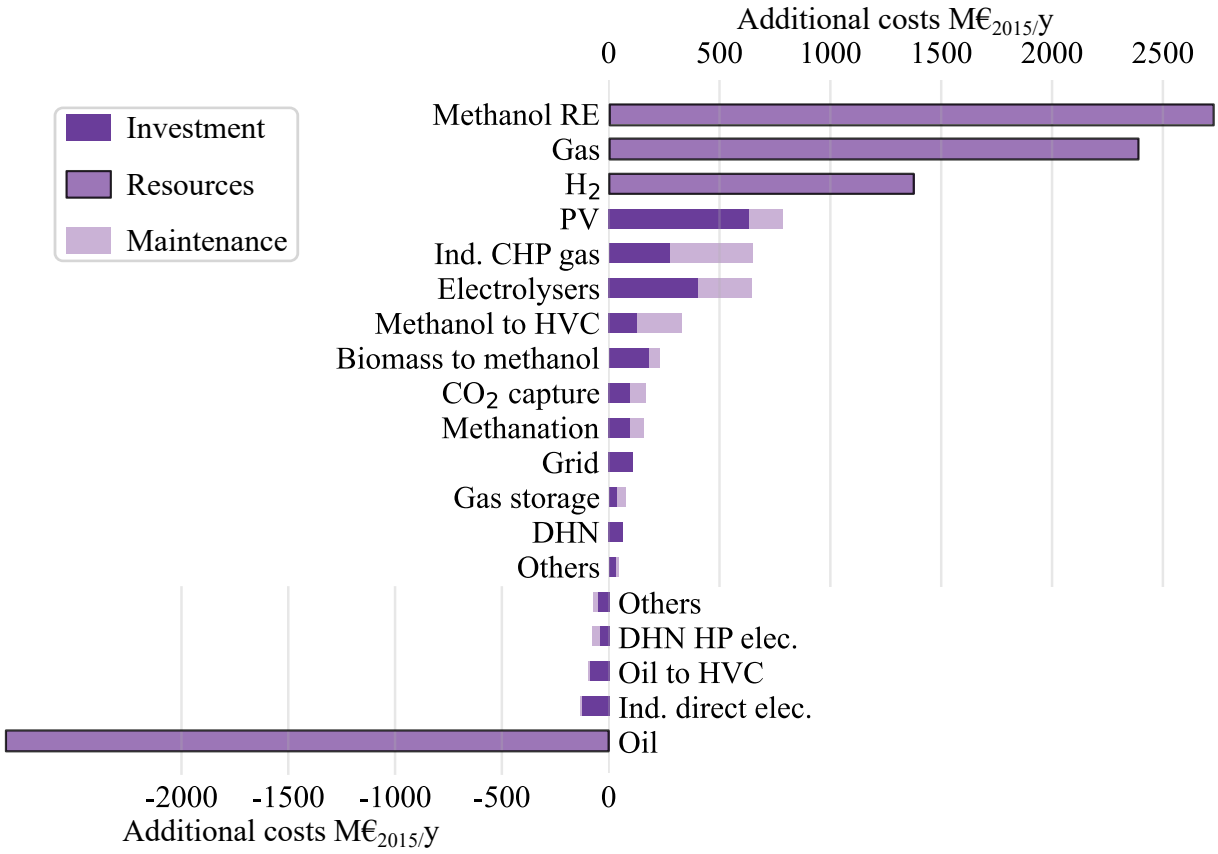

Figure 3.6: The breakdown of the additional costs relative to the case with no power-to-gas indicates the origins of the 6.5 b€$_{2015}$/y difference of total cost. Abbreviations: renewable (RE), photovoltaic (PV), industrial (ind.), combined heat and power (CHP), heat pump (HP), high-value chemicals (HVC), district heating network (DHN).

the CO_2 emissions of the port of Antwerp are relatively small.

A focus on the costs differences outlines the differences in the energy system (Figure 3.6). First, the significant raise of importations of H_2, natural gas and renewable methanol contributes the most to the additional expenses. The importations are favoured as they are cheaper than producing domestically these energy carriers. Second, as discussed previously, the installed capacity of PV panels, of industrial CHP plants fueled with gas, of the technologies making up the PtG system and of the production of HVC with methanol increases and so do the costs associated with them.

The DHN and the electricity network also imply extra costs. The electricity grid is reinforced due to the integration of more intermittent renewable energy which is here the PV panels. The DHN is proportional to the capacity of the technologies producing the corresponding heat. Consequently, the heat for the DHN generated by the electrolysers and the methanation implies a bigger DHN which results in extra costs. The production of this heat outweighs the reduced

heat generated by the heat pumps.

The others category includes all the costs differences lesser than 50 M€$_{2015}$/y. For the extra costs, this category comprises the costs related to the CO_2 storage and to the industrial boilers fueled with gas and waste. For the negative additional costs, it includes thermal storage at high temperature, the CCGTs and the biomass boilers.

The gas and CO_2 storage raise because the production of gas, captured CO_2 and heat at low temperature for the DHN is greater. In fact, with no storage the installed capacity of a technology corresponds to its peak production. Therefore, the capacity of the technology is oversized which leads to higher costs. The storage technologies buffer the peak production and limit then the installed capacity. Surprisingly, the opposite occurs for the waste boilers. The installed capacity is greater than in the reference case, whereas the energy balance over the year stays the same. It means that the capacity of the waste boilers is oversized. Accordingly, the capacity of the thermal storage at high temperature decreases. The share of the heat at high temperature generated by the gas boilers increases in spite of the biomass boilers. The reason is that biomass is almost fully dedicated to the production of methanol. As a reminder, the methanol production significantly raises with PtG in the port because methanol instead of oil is used for the production of HVC. Hence, the heat at high temperature generated by the biomass boilers in the reference case is rather produced by gas boilers. The production of gas boilers also offsets the one of direct electricity heating.

Finally, the costs differences related to the CCGTs are *a priori* unexpected. While the production of electricity by CCGTs increases significantly (Figure 3.4), the installed capacity is lower with the post-combustion capture and slightly higher with the oxy-fuel combustion capture. Let's first focus in the case with post-combustion to understand what is going on. As shown in Figure 3.5, more gas is available with PtG in the port of Antwerp. In this case, the capacity factor of the CCGTs rises from 0.12 to 0.86. Moreover, the peak production is reduced. These two factors lead to a bigger production while keeping a limited installed capacity, and thus reduced costs. For oxy-fuel combustion capture, the capacity factor remains high, but the bigger electricity production by CCGT compared to post-combustion capture results in a slightly higher peak production than in the reference case. Therefore, the installed capacity and thus the costs are also slightly higher in this case[8].

[8] The figure with the detailed additional costs for oxy-fuel combustion capture is available in Appendix D.2.

3.3 Partial utilisation of the captured CO_2

In this scenario, the projection of the quantity of hydrogen that could be used for the hydrogenation of the CO_2 in 2030 is set as input. The estimation amounts to 11 TWh_{H_2} from importations and 0.65 TWh_{H_2} domestically produced which gives a total of 11.65 TWh_{H_2}. A part of the captured CO_2 thus reacts with this hydrogen, while the other is sent for long-term storage.

This section aims to verify if this scenario is energetically more feasible than utilising all the CO_2. As post-combustion capture consumes more specific energy than oxy-fuel combustion capture, this capture technology is more critical in terms of energy. Therefore, only post-combustion capture is considered for the following results. With oxy-fuel combustion capture, the results would have been very similar. Due to the specific energy consumption differences and as the quantity of CO_2-rich stream captured is slightly higher with this latter capture technology, it would have just resulted in a bit more CO_2 stored and minor differences in the energy consumption and production.

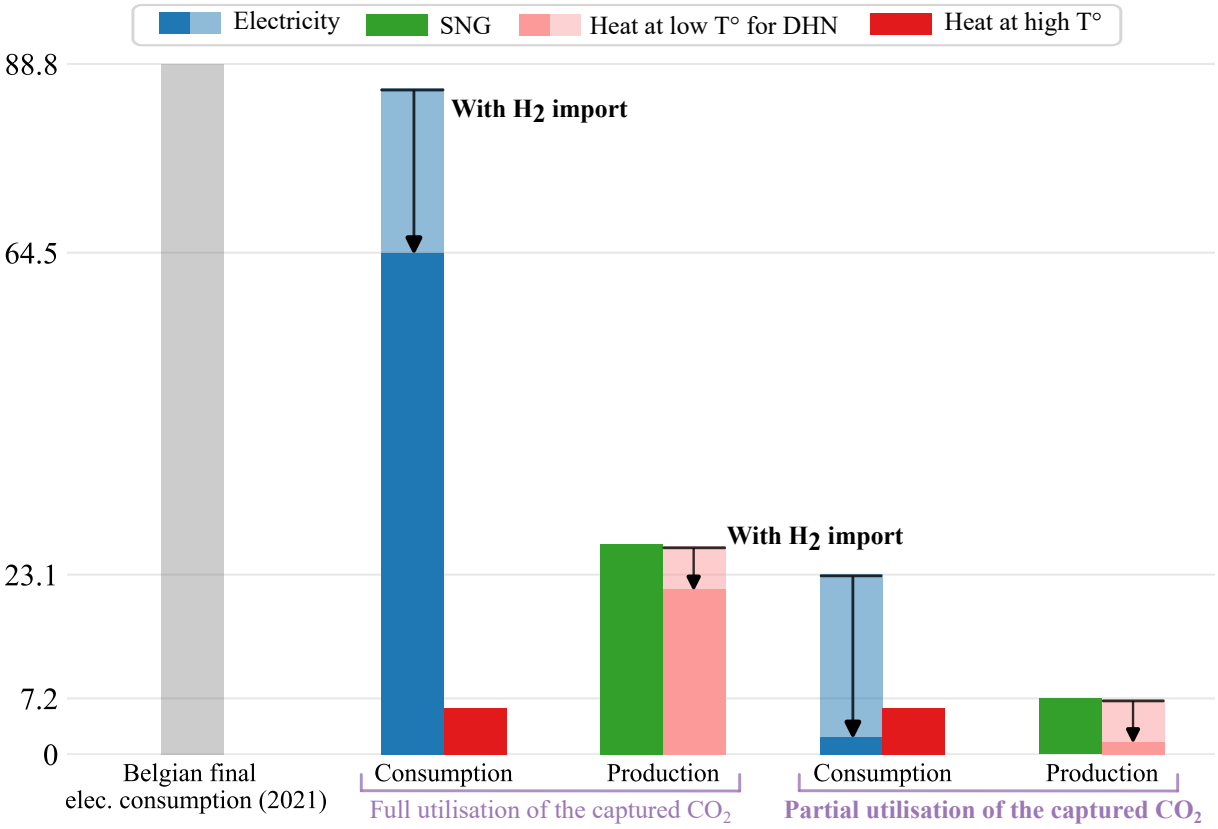

Figure 3.7: Comparison of the energy consumption and production between using 26.4% (1.9 Mt_{CO_2}) of the captured CO_2 (on the right) and using all the captured CO_2 (on the left). The capture technology used is the post-combustion capture. Abbreviations: synthetic natural gas (SNG), district heating network (DHN), electricity (elec.).

As a reminder, 7.2 Mt_{CO_2} are captured with this capture system. Among this CO_2, 5.3 Mt_{CO_2} (73.6%) are then going to be stored and 1.9 Mt_{CO_2} (26.4%) are going to be used, which outcomes in 7.19 TWh_{SNG} produced by methanation.

With 11 TWh_{H_2} imported, the domestic hydrogen production decreases of 98 % compared to the full utilisation scenario (Figure 3.7). Therefore, even if the energy requirement for the CO_2 capture stays the same, a significant drop of electricity consumption (97%) is expected as the electrolysers contribute the most to the electricity consumption. On the other side, the total energy production naturally falls from 43.7 TWh to 7.5 TWh.

As outlined before, the energy requirement for the CO_2 capture is minor compared to the electrolysers consumption. Therefore, the changes in the electricity mix are relatively small when the quantity of used CO_2 matches the projections of available hydrogen for the methanation (Figure 3.8).

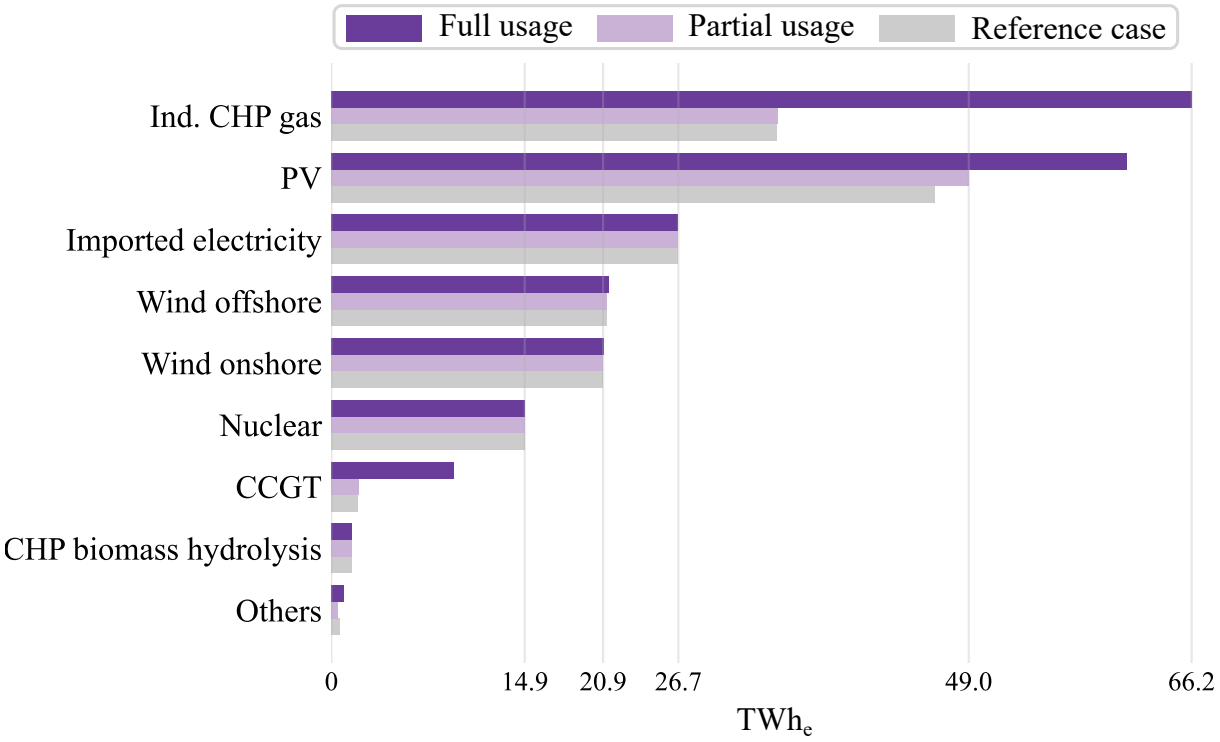

Figure 3.8: Comparison of the electrical mix between a partial utilisation, a full utilisation of the captured CO_2 and the case with no power-to-gas in the port of Antwerp. The capture technology used is the post-combustion capture. Abbreviations: photovoltaic (PV), industrial (ind.), combined heat and power (CHP), combined cycle gas turbine (CCGT).

In this scenario, the PV production also raises, but the installed size (47.8 GW) is closer to the reference case (45.3 GW). The industrial gas CHP and the CCGT production is still bigger, despite a tiny difference. Then, the optimisation performed by ESTD results in an installed

capacity of the electrolysers of 394 MW (together with a small capacity factor of 0.22) which is way more than the foreseen 150 MW.

The others category still includes the hydropower plants and conversion technology of biomass to methanol. However, the production of electricity via the latter declines this time[9].

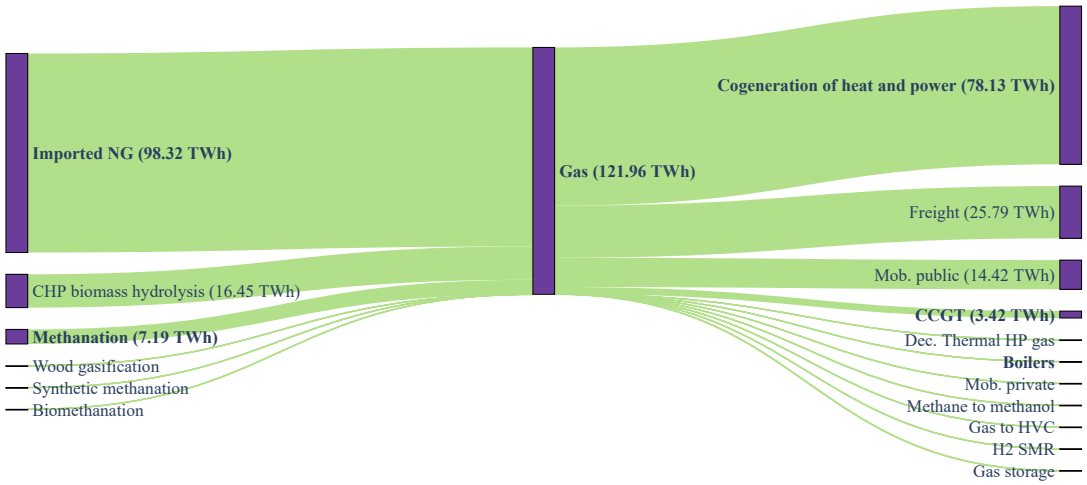

(a) Case with partial utilisation of the captured CO_2 in the port with post-combustion capture.

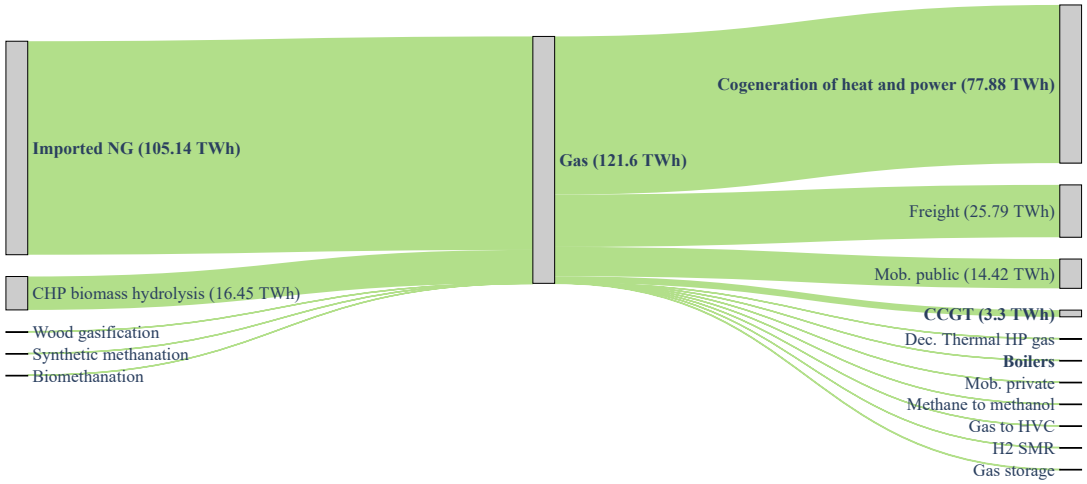

(b) Case without power-to-gas in the port of Antwerp.

Figure 3.9: The comparison of the gas flows between case (a) and (b) indicates a decrease of the natural gas import with power-to-gas in the port of Antwerp. Gas naming refers to either natural gas or synthetic natural gas. Names in bold emphasise the differences between the reference case and the case with the partial utilisation of the captured CO_2. Abbreviations: imported (imp.), natural gas (NG), combined heat and power (CHP), combined cycle gas turbine (CCGT), decentralised (dec.), heat pump (HP), mobility (mob.), high-value chemicals (HVC), steam methane reforming (SMR).

In conclusion, this scenario is more realistic in terms of energy consumption, but it is based on a big estimation of the future hydrogen import. In Europe, the current capacity of installed

[9]The explanation of this difference will be clearer after discussing the Sankey diagrams (Figure 3.9).

electrolysers amounts to 160 MW [79]. As Belgium expects an electrolyser capacity of 150 MW by 2030, it means that strong investments are needed to reach the objective.

The quantity of available gas is almost the same between the two cases (Figure 3.9). Nonetheless, the natural gas imports are lower in the partial utilisation case as the SNG production by methanation fills the gap. The slight additional gas supplies the CHP plants and the CCGTs.

As the imported gas goes down of 6.82 TWh, the GHG emitted by the gas combustion are lower in the partial utilisation case, even if the quantity of available gas is slightly higher. In compensation, more light fuel oil, instead of methanol, is consumed for the production of HVC. Therefore, less methanol is produced and hence, the lower generation of electricity via the production of methanol with biomass.

3.4 Sensitivity analysis

Until now, all results shown and discussed were nominal values. However, these results are sensitive to the uncertainty going along with the parameters described in Section 2.9. This section aims to analyse the impacts of those parameters on the results.

3.4.1 Energy system

In Section 3.1.3, it was reported that without constraining the operation of the PtG technologies in the model, none of these technologies are installed. The GWP limit has been decreased to 0 $kt_{CO_2,eq}/y$, but still no installation is observed. It should be kept in mind that the model does not take into account the captured CO_2 in the CO_2 emissions accounting. It thus means that these technologies are not economically optimal for the energy system. The costs of the technologies have then been reduced to the lower range. Even at these costs, the optimisation results in no captured CO_2. As no cost range for the capture technology has been considered, the investment and maintenance cost of this technology have been decreased by applying factors below 1 to the costs. Still, even at costs of the capture technology being 4 times lower, no installation is realised.

Even though this set of technologies is not optimal for the model, in reality, CCU and CCS are necessary to decarbonise hard-to-abate industries such as the ones in the port of Antwerp.

In Figure 3.10, the error bar underlines the difference of specific energy consumption of the ASU if all the oxygen is supplied by the ASU or by the electrolysers and represents a variation

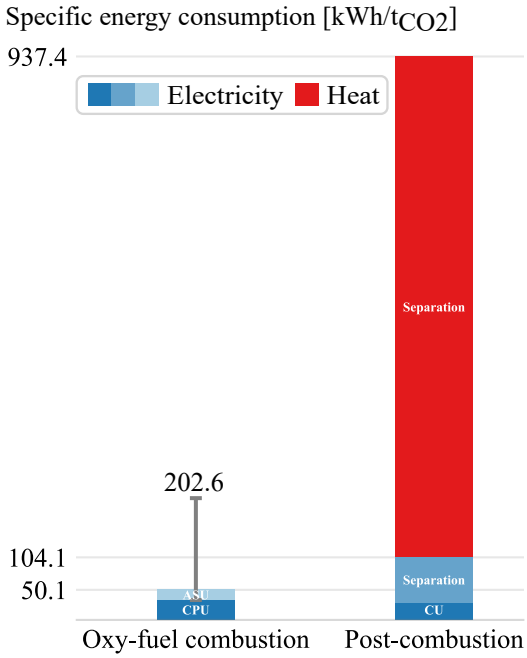

Figure 3.10: The breakdown of the specific energy consumption of the capture technologies when considering no or all the oxygen produced by the air separation unit indicates a variation of +304% and -34% of the specific energy consumption. Blue colours refer to electricity and red colour refers to heat. Abbreviations: air separation unit (ASU), compression and processing unit (CPU), compression unit (CU).

of specific electricity consumption of +304% and -34%. The case where all the oxygen would be supplied by the electrolysers is an ideal, but unlikely scenario for two main reasons. First, it is expected that Belgium will rely on hydrogen imports to meet its hydrogen demand. Consequently, the oxygen would need to be imported, increasing the logistic and economic limitations. Second, the hydrogen production will not be steady and continuous. In fact, water electrolysis will be performed during high renewable energy production. Though, a constant oxygen supply is required for the combustion to keep on capturing the CO_2. The case where all the oxygen is produced with the ASU leads to a significant specific energy consumption raise as this latter is energy-intensive. Nonetheless, the total specific energy consumption of post-combustion capture remains 4.6 times higher than oxy-fuel combustion capture.

In the case of full utilisation of the captured CO_2, the products are determined by the quantity of CO_2 used. The estimated CO_2 emissions in the port of Antwerp reach up to 17 Mt_{CO_2}/y [5], corresponding to 18.8% of the total CO_2 emissions of Belgium in 2019. Setting the 14.3 Mt_{CO_2}/y as the base value, a range of CO_2 emissions is defined from 11.7 Mt_{CO_2}/y to 17 Mt_{CO_2}/y. As this study focuses on halving the emissions, it gives a span of 5.85 Mt_{CO_2} to 8.5 Mt_{CO_2}. In the partial utilisation case, the quantity of hydrogen used is the input. The assumed range of the hydrogen demand for the methanation begets 8 TWh to 14 TWh of hydrogen im-

ported, and 0.47 TWh to 0.83 TWh are domestically produced. The uncertainty of the input of these both cases is analysed (Figure 3.11). In both cases, the H_2 import is taken into account in the energy consumption and production.

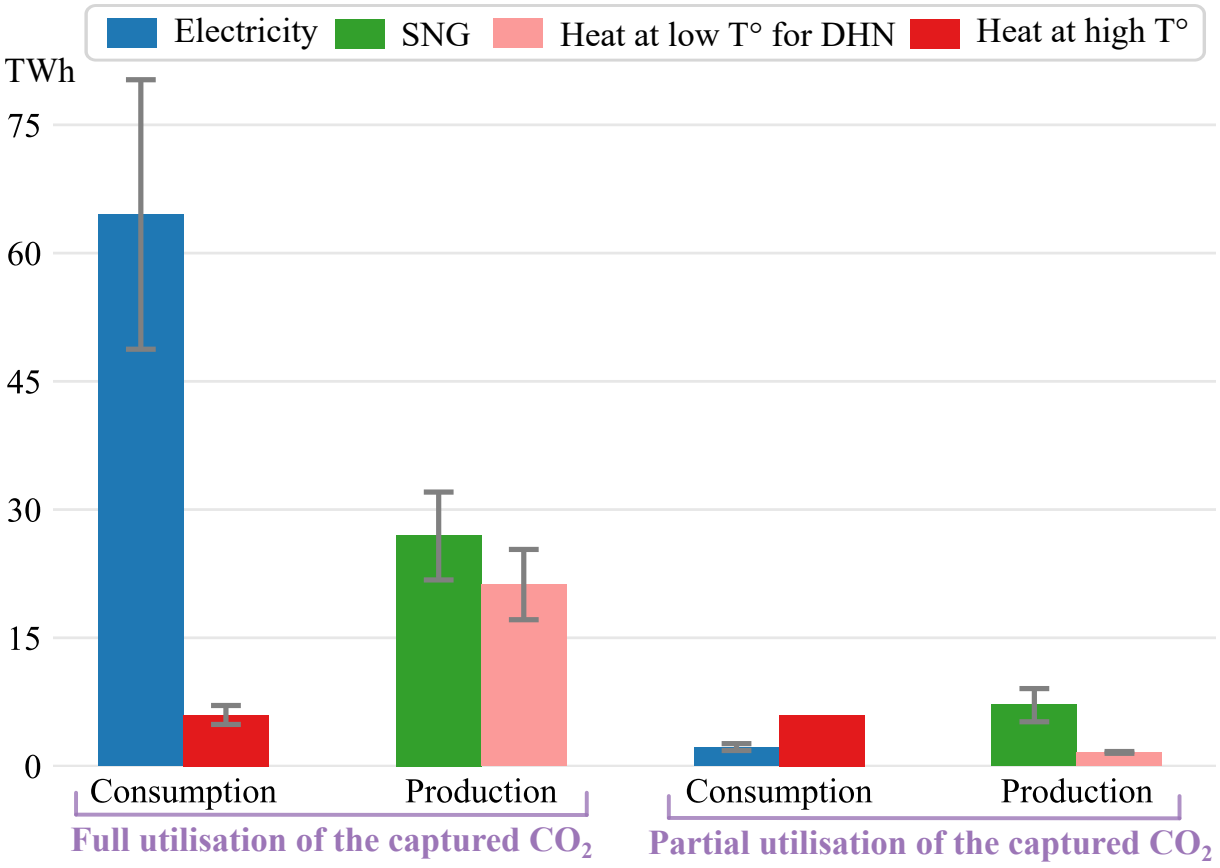

Figure 3.11: Sensitivity of the energy production and consumption of a power-to-gas system depending on a range of captured CO_2 (5.8 Mt_{CO_2} to 8.5 Mt_{CO_2}) on the left and the future hydrogen availability for the methanation on the right (40% to 70%). Abbreviations: synthetic natural gas (SNG), district heating network (DHN), electricity (elec.).

When all the captured CO_2 is used, the production of SNG amounts to between 21.8 TWh_{SNG} and 32 TWh_{SNG} and generates from 17.1 TWh_{th} to 25.3 TWh_{th}. It corresponds to an electricity consumption of 48.8 TWh_e to 80.3 TWh_e and a heat need of 4.9 TWh_{th} to 7 TWh_{th}. In the partial utilisation case, the variation is lower, resulting in 5.18 TWh_{SNG} to 9.1 TWh_{SNG} and from 1.5 TWh_{th} to 1.7 TWh_{th} produced. Concerning the consumption, the one for the capture does not change, but the variation of hydrogen domestically produced leads to a range from 1.8 TWh_e to 2.8 TWh_e.

In the partial utilisation case when considering both uncertainties, the amount of CO_2 used reaches 41.6% with the lower limit of CO_2 emissions and the upper one of hydrogen projection and 16.3% of the captured CO_2 with the opposite limits.

3.4.2 Economic analysis

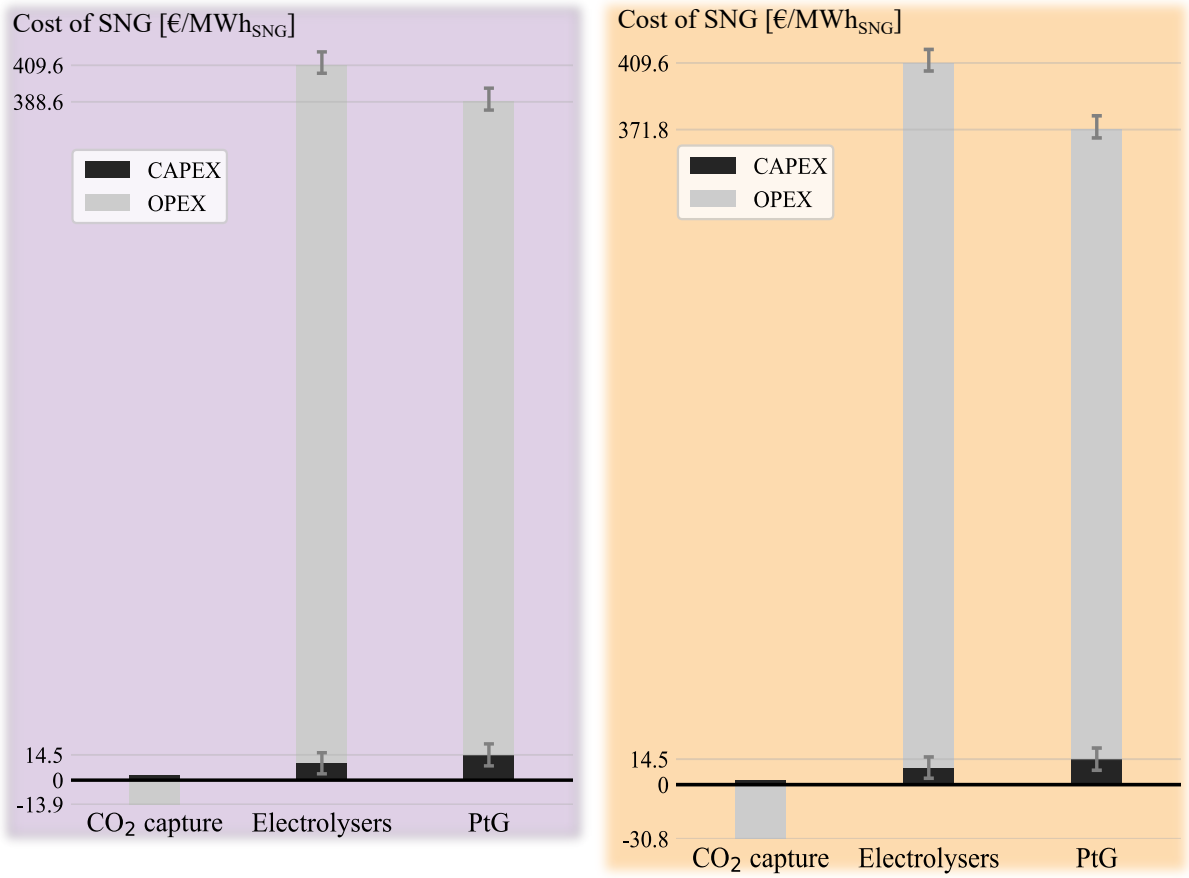

(a) Post-combustion capture.

(b) Oxy-fuel combustion capture.

Figure 3.12: The sensitivity analysis of the investment and maintenance cost on the breakdown of the levelised cost of synthetic natural gas indicates their small impact on the LCSNG. The other sensitive parameters as the electricity price are not included.

Despite a wide range of investment cost and maintenance cost, their impact on the LCOE is relatively low (Figure 3.12). In fact, the LCSNG only varies of +3.6% and -2.8% and +3.8% and -3% between the mean for post and oxy-fuel combustion capture. This range will shrink as the maturity and the development of projects will raise. As the LCSNG is clearly driven by the operation rather than the CAPEX, improvements in the technologies would result in a lower consumption, and thus, a lower OPEX. Choosing technologies with a low specific consumption rather than a low CAPEX seems then being a better option. To investigate what impacts the operation cost the most, a two parameters analysis has been performed with the two highly volatile parameters: the electricity price and the carbon price (Figure 3.13).

The evolution of the LCSNG for carbon prices between 80 €/t$_{CO_2}$ and 129 €/t$_{CO_2}$ and for the two capture systems lies in between the two illustrated lines as it has been shown that post-

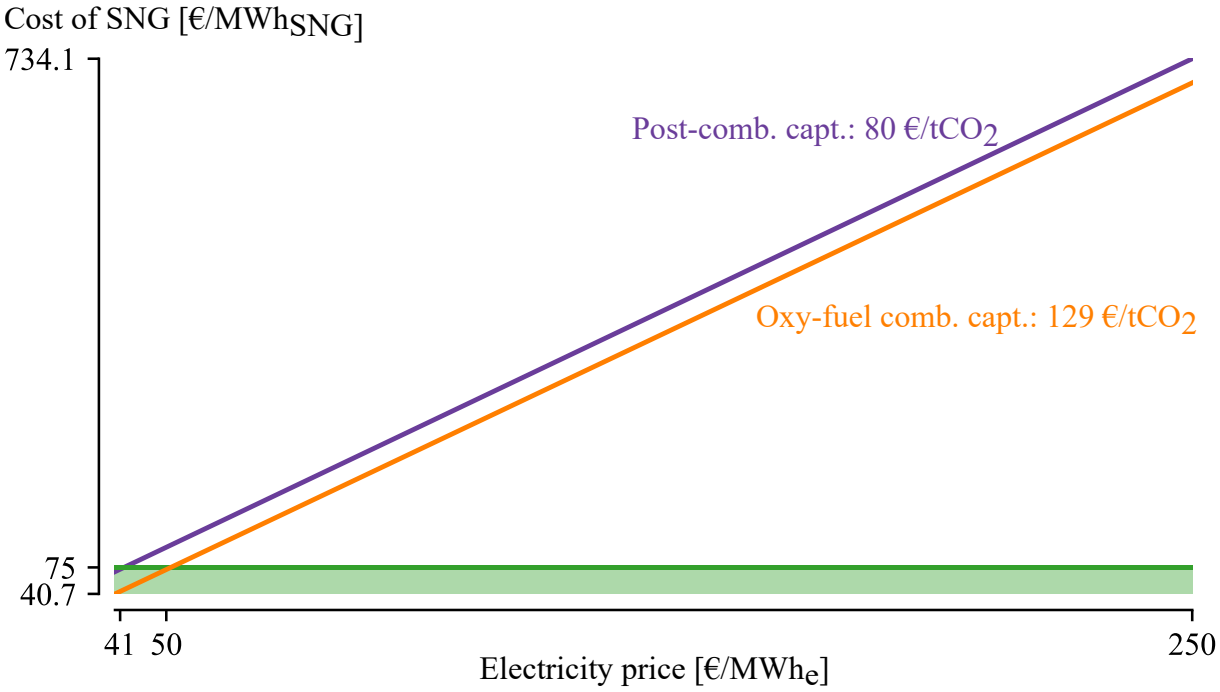

Figure 3.13: The levelised cost of synthetic natural gas depending on the electricity price and the CO_2 price indicates that at an electricity price between 41 €/MWh_{SNG} and 50 €/MWh_{SNG}, power-to-gas becomes economically attractive. Abbreviations: synthetic natural gas (SNG), combustion (comb.) and capture (capt.).

combustion capture is slightly more expensive than oxy-fuel combustion capture. The LCSNG covers a span from 40.7 €/MWh_{SNG} to 734.1 €/MWh_{SNG}. This range is in line with the study of Coppitters *et al.* [53] on a a direct air capture integrated with the CO_2 methanation, as they reported a LCSNG from 130 €/MWh_{SNG} to 744 €/MWh_{SNG}. The electricity price affects more the LCSNG than the carbon price due to the massive electricity consumption of the electrolysers. Hence, even if a high CO_2 price is important for the transition, the economic viability depends more on the electricity price. Gorre *et al.* [46] define a price of SNG in 2030 to 75 €/MWh_{SNG}. This price is higher than the projection of the natural gas price made by the European Commission (30 €/MWh_{SNG}) for 2030. Economic incentives are then required to foster this change. Depending on the carbon price, the business becomes attractive at an electricity price between 41 €/MWh_e and 50 €/MWh_e which is in line with Gorre *et al.* [46], considering the volatility of the electricity price. In fact, they found out that PtG becomes profitable at a price of 24 €/MWh_e. Policies and economic incentives are thus needed to enhance the development of PtG projects.

The uncertainty of the total cost is studied in the case of the full utilisation of the captured CO_2 with post-combustion capture (Figure 3.14)[10]. The range of the quantity of captured CO_2 involves a variation of +3.8% and -3.2% of the total cost, while the costs uncertainty of the tech-

[10]The illustration for the oxy-fuel combustion capture is shown in Appendix D.2.

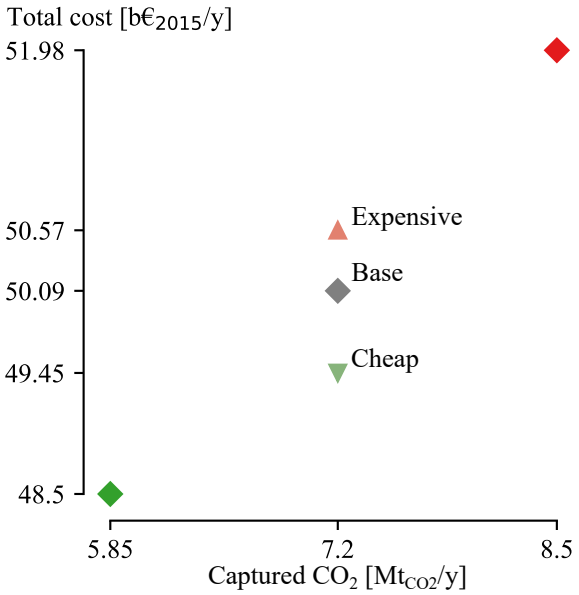

Figure 3.14: The uncertainty related to the quantity of captured CO_2 leads to a variation of +3.8% and -3.2% of the total cost, which is more than with the technologies costs on the lower limit (cheap scenario) and the upper limit (expensive scenario). The total cost corresponds to the full utilisation of the CO_2, captured by post-combustion capture. All the diamond markers refer to the base costs.

nologies involves a change of +0.9% and -1.3%. Compared with the reference case, it means a costs difference of 4.9 to 8.4 b€$_{2015}$/y which corresponds to an increase between 11% and 19%. Then, it is noted that the higher the amount of captured CO_2, the higher the total cost and vice versa. It is explained by the fact that the greater amount of captured emissions increases the installed size of the capture technology, and because it also increases the energy requirement. These two factors lead to higher costs. In the cheap scenario, the production of hydrogen by the electrolysers becomes more attractive. However, the large hydrogen demand in the full utilisation case still begets a maximum H_2 import. As the technologies are cheaper, the model sizes them to the peak production which means that the technologies of the PtG are oversized. In other words, the installed capacity is greater in the cheap scenario than with the base cost, whereas the operation of the PtG remains the same. Though, the resulting costs of the PtG are lower. These changes imply a lot of changes in the energy system, but overall, the cheap scenario results in a lower total cost, as expected. In the expensive scenario, the opposite occurs. The installed size is minimised to lower the induced costs and hence, the capacity factor is maximised.

Chapter 4

Conclusion

The port of Antwerp emits between 14.34 Mt_{CO_2} and 17 Mt_{CO_2} which represents 15.9–18.8% of the total CO_2 emissions in Belgium in 2019. The decarbonisation of this chemical cluster is thus crucial to meet the 2030 emissions target of Belgium. Though, capturing this amount of CO_2 and finding the optimised way of handling this CO_2 is not straightforward.

Oxy-fuel and post-combustion capture have been selected as the best methods to capture CO_2 in the port. In terms of specific energy requirement, the uncertainty of the quantity of O_2 produced by the ASU results in a consumption of 33.11–202.6 kWh/t_{CO_2} for oxy-fuel combustion capture. Despite this wide range, post-combustion capture still requires 4.6 to 18.7 times more energy, mainly due to the large heat requirement for the regeneration of the MEA solvent. Therefore, one could conclude that oxy-fuel combustion capture is a better method, but the specific energy consumption does not represent the big picture. In fact, the easiness of retrofitting an existing facility for the capture and the related costs are key factors too. On this point, post-combustion capture is the preferred option.

Due to its greater energy need, PtG with post-combustion capture is a bit more expensive. Overall, the LCSNG varies from 40.7 €/MWh_{SNG} to 734.1 €/MWh_{SNG}. The electricity price has a major impact on the LCSNG due to the massive electricity production of the electrolysers. With an estimated price for SNG of 75 €/MWh_{SNG} in 2030, PtG becomes cost-effective at electricity price between 41 €/MWh_e and 50 €/MWh_e. The uncertainty of the investment and operation cost only changes the nominal LCSNG of maximum +3.8% and -3%. As the operation drives the LCSNG rather than the costs of the technologies, choosing technologies with a low specific consumption seems to be a better option. Economic incentives and policies are required to make PtG more profitable and help the port to comply with its target.

Once the PtG system implemented on ESTD, it is concluded that PtG is not optimal for the energy system according to the model, even with a GWP limit of 0 kt_{CO_2} and costs at the lower limit. However, the model does not consider that CO_2 is captured when accounting the GHG emissions. This a weakness in the model which can be corrected by modifying the model so that the captured CO_2 is accounted in the GWP.

To analyse the impacts of using and storing the CO_2, two scenarios have been defined by constraining the model to install the PtG technologies: utilising all the captured CO_2 for the methanation or utilising only the CO_2 needed to react with all the available H_2 for the methanation. The rest of the captured CO_2 is then stored permanently underground.

With post-combustion capture, the full utilisation scenario results in additional costs of 4.9–8.4 b€$_{2015}$/y which corresponds to an increase between 11% and 19% compared to the case without CCU in the port of Antwerp. It means that 1.2% of the gross domestic product of Belgium in 2022 is spent additionally each year. Knowing that the floods of 2021 in Belgium cost 2.5 b€ according to the annual report of Assuralia, the additional costs for the transition in the port of Antwerp are relatively small. Utilising all the captured CO_2 leads to a production of 21.8–32 TWh_{SNG} and 17.1–25.3 TWh_{th} depending on the amount of captured CO_2 assumed. As the optimisation of the model entails a maximum H_2 import (11 TWh), it corresponds to an electricity consumption of 48.8–80.3 TWh_e and a heat need of 4.9–7 TWh_{th}. This electricity is produced partially by installing the maximum achievable capacity of PV (59.2 GW) and 10 GW of electrolysers need to be installed to reach the required production of hydrogen. To put it in perspective, Europe has currently an installed capacity of electrolysers of 160 MW. Undoubtedly, deploying such a massive capacity of PV and electrolysers by 2030 is unrealistic. The rest of the additional energy production comes mainly from the CCGTs and the industrial CHP fueled with gas. Overall, 69.6% more gas is consumed in this case. The gas produced by the methanation is not enough to outweigh this gas consumption. Therefore, the gas import increases from 105.14 TWh to 162.74 TWh. In conclusion, while this scenario results in realistic additional costs, such an energy system is unachievable by 2030.

In the partial utilisation case, 5.18–9.1 TWh_{SNG} are produced using 8–14 TWh of imported hydrogen and 0.47–0.83 TWh produced domestically, depending on the ratio of the hydrogen demand for the methanation (40% to 70%). In addition, when taking into account the potential range of captured CO_2, between 16.3% and 41.6% of CO_2 is used. This domestic hydrogen production leads to an important diminution of the electricity need compared to the previous scenario. The installed capacity of PV panels is then more realistic, and the imported natural gas is, this time, lower than the reference case. Therefore, using part of the captured CO_2 and storing the rest is more realistic.

It is worth mentioning that the conclusions drawn with post-combustion capture are the same than with oxy-fuel combustion capture.

Appendices

Appendix A

Sectors included in the Regulation 166/2006

The table below shows the sectors included in the E-PRTR and their respective code which are used in the database (Table A.1).

Table A.1: Sectors included in the European Pollutant Release and Transfer Register and their corresponding code [24].

Sector names	Code
Energy sector	1
Production and processing of metals	2
Mineral industry	3
Chemical industry	4
Waste and wastewater management	5
Paper and wood production and processing	6
Intensive livestock production and aquaculture	7
Animal and vegetable products from the food and beverage sector	8
Other activities	9

Appendix B

Energy system implementation

An overview of the matrix implemented in ESTD which defines the outputs (positive values) and the inputs (negative values) of the technologies added in the model, is shown in Table B.1. The energy carriers or resources are the rows and the conversion technologies are the columns. Each output and input are expressed by unit of the main output. This latter is defined as the resource with a 1 (positive or negative) for each technology. Hence, all the layers interacting with the CO_2 capture technology are expressed in kt_{CO_2}, while the other layers are in GWh. When the column has no connection with a layer, the corresponding matrix element is filled with no value. It is noted that in the matrix, the geological storage only consumes captured CO_2, which is equivalent to store permanently the CO_2. No energy consumption has been assumed for this technology because it is too case specific.

Table B.1: Consumption and production matrix. The values for post-combustion capture are in purple and the ones for oxy-fuel combustion capture are in orange.

	CO_2 capture	PEME	Methanation	Geological sto.
Electricity	-0.09 -0.05	-1.92	-	-
H_2	-	1	-1.64	-
Gas	-	-	1	-
Heat at high T°	-0.73 -	-	-	-
Heat at low T°	-	0.5	0.17	-
CO_2 Antwp.	-1	-	-	-
Captured CO_2	0.88 0.99	-	-0.27	-1

[a] All the energy carriers are expressed in GWh, expect the CO_2 which is in kt_{CO_2}.

[b] Abbreviations: proton exchange membrane electrolyser (PEME), storage (sto.), Antwerp (Antw.).

Appendix C

Economic analysis

C.1 Conversion of the currencies and their year of reference

All the costs are expressed in $€_{2015}$. The costs referring to another year or expressed with another currency are all converted by Eq. C.1:

$$c\left[€_{2015}\right] = c\left[C_{\mathrm{y}}\right] \cdot \frac{USD_{\mathrm{y}}}{C_{\mathrm{y}}} \cdot \frac{CEPCI_{2015}\left[USD_{2015}\right]}{CEPCI_{\mathrm{y}}\left[USD_{\mathrm{y}}\right]} \cdot \frac{€_{2015}}{USD_{2015}} \tag{C.1}$$

where c refers to any cost, C is the original currency which is converted to euro, y is the year of the original currency, USD stands for United States dollar and CEPCI is the Chemical Engineering Plant Cost Index (CEPCI). The CEPCI has been introduced to take into account the evolution of the production costs. As it is based on USD, a conversion is first performed from the original currency to USD and then, to €. Although this index is proposed for plants, its utilisation has been extended to resources [34, 80]. The CEPCI from 1990 to 2020 are listed in Table C.1:

Table C.1: Chemical Engineering Plant Cost Indexes (CEPCI) from 1990 to 2020 [80].

Year	CEPCI
1990	357.6
1991	362.3
1992	367.0
1993	371.7
1994	376.4
1995	381.1
1996	381.7
1997	386.5
1998	389.5
1999	390.6
2000	394.1
2001	394.3
2002	395.6
2003	402.0
2004	444.2
2005	468.2
2006	499.6
2007	525.4
2008	575.4
2009	521.9
2010	550.8
2011	585.7
2012	584.6
2013	567.3
2014	576.1
2015	556.3
2016	541.7
2017	567.5
2018	603.1
2019	607.5
2020	594.1

C.2 Levelised Cost of Synthetic Natural Gas

The Levelised Cost of Synthetic Natural Gas (LCSNG) depends on multiple technologies. Each technology are multi-resources and multi-outputs. The definition of the levelised cost of electricity, proposed in Gauthier Limpens'thesis, is defined for single resource and single output technologies, and is therefore adapted [34].

The technologies comprised in the PtG system are grouped in a set named *PtG TECHS*. The set of resources (referred as *RES*) and of sold products (*SOLD PROD*) of each technology in *PtG TECHS* are resumed in Table C.2.

Table C.2: Set of technologies included in power-to-gas, of the resources and of the sold products, considered in the computation of the levelised cost of synthetic natural gas.

PtG TECHS	*RES*	*SOLD PROD*
Capture technology		
Post-combustion capture	Electricity, heat at high T°	CO_2
Oxy-fuel combustion capture	Electricity	CO_2
Electrolyser	Electricity, water	Heat at low T°
Methanation unit	-[a]	Heat at low T°

[a] H_2 and CO_2 resources for methanation are not accounted in the LCOE of methanation, as the cost of these resources is accounted in the LCOE of the electrolyser and the CO_2 capture.

The LCOE is computed as the sum of the CAPEX related LCOE and the OPEX LCOE. The OPEX LCOE of each technology depends on their respective resources and sold products considered. Their formula is developed as follows:

$$LCO\,CO_{2,\text{opex}}\left[\frac{€}{t_{CO_2}}\right] = c_{\text{op}}(elec.)f(capt.,elec.) + \overbrace{c_{\text{op}}(HHT)f(capt.,HHT)}^{\text{if post-combustion capt.}} - \text{CO}_2 price + \frac{c_{\text{maint}}}{c_{\text{p,expected}} \cdot 8760} \quad \text{(C.2)}$$

$$LCO\,H_{2,\text{opex}}\left[\frac{€}{\text{MWh}_{H_2}}\right] = c_{\text{op}}(elec.)f(electro.,elec.) + c_{\text{op}}(water)f(electro.,water) - c_{\text{op}}(HLT)f(electro.,HLT) + \frac{c_{\text{maint}}}{c_{\text{p,expected}} \cdot 8760} \quad \text{(C.3)}$$

$$LCO\ SNG_{\text{opex}}\ \left[\frac{€}{\text{MWh}_{\text{SNG}}}\right] = -c_{\text{op}}(HLT)\,f\,(metha., HLT) + \frac{c_{\text{maint}}}{c_{\text{p,expected}} \cdot 8760} \qquad \text{(C.4)}$$

where HHT stands for Heat at High Temperature, HLT stands for Heat at Low Temperature, elec. for electricity, capt. for capture technology, electro. for electrolyser and metha. for methanation. *f(tech, res)* is defined as the amount of resource (*res*) required by unit of the main output of technology (*tech*). Same logic is applied to *f(tech, prod)*. For instance, from Section 2.2.2, *f(electro., HLT)* = 16.68 $\text{kWh}_{\text{th}}/\text{kg}_{\text{H}_2}$ which is converted to the right unit.

Finally, the OPEX LCOE and CAPEX LCOE of each technology are summed and the LCSNG is obtained by Eq. C.5:

$$LCSNG\ =\ LCO\ CO_2 \cdot f\,(metha., \text{CO}_2)\ +\ LCO\ H_2 \cdot f\,(metha., \text{H}_2)\ +\ LCO\ SNG \qquad \text{(C.5)}$$

Appendix D

Results for oxy-fuel combustion capture

D.1 Gas flows

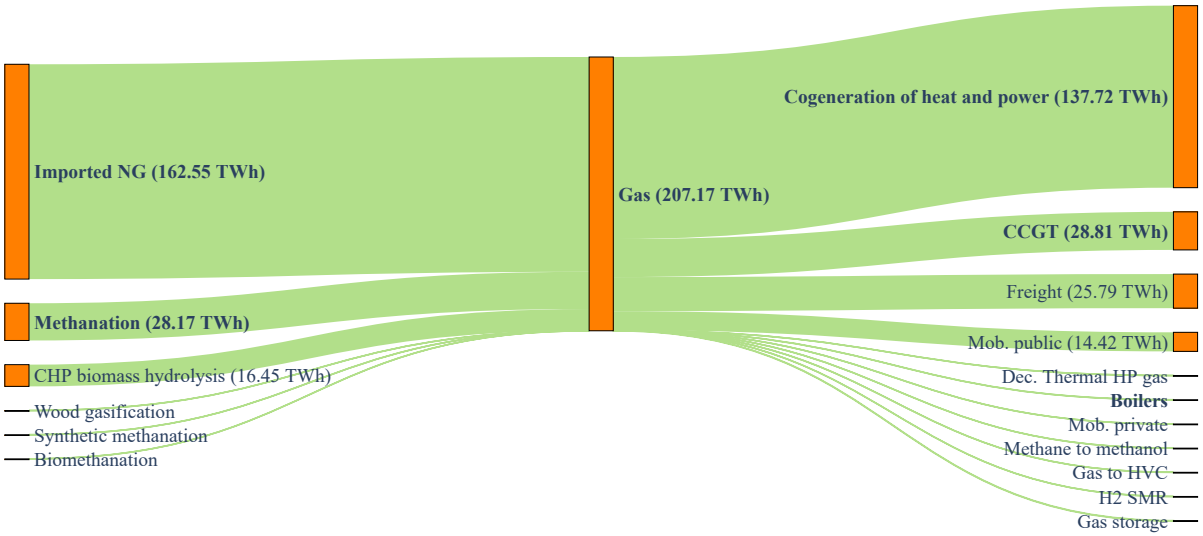

Figure D.1: Gas flows in the energy system from its origin to its consumption with a power-to-gas system with oxy-fuel combustion capture. *Gas* naming refers to either natural gas or synthetic natural gas. Names in bold emphasise the differences between the reference case and the case with the utilisation of the captured CO_2. Abbreviations: imported (imp.), natural gas (NG), combined heat and power (CHP), combined cycle gas turbine (CCGT), decentralised (dec.), heat pump (HP), mobility (mob.), high-value chemicals (HVC), steam methane reforming (SMR).

D.2 Costs difference

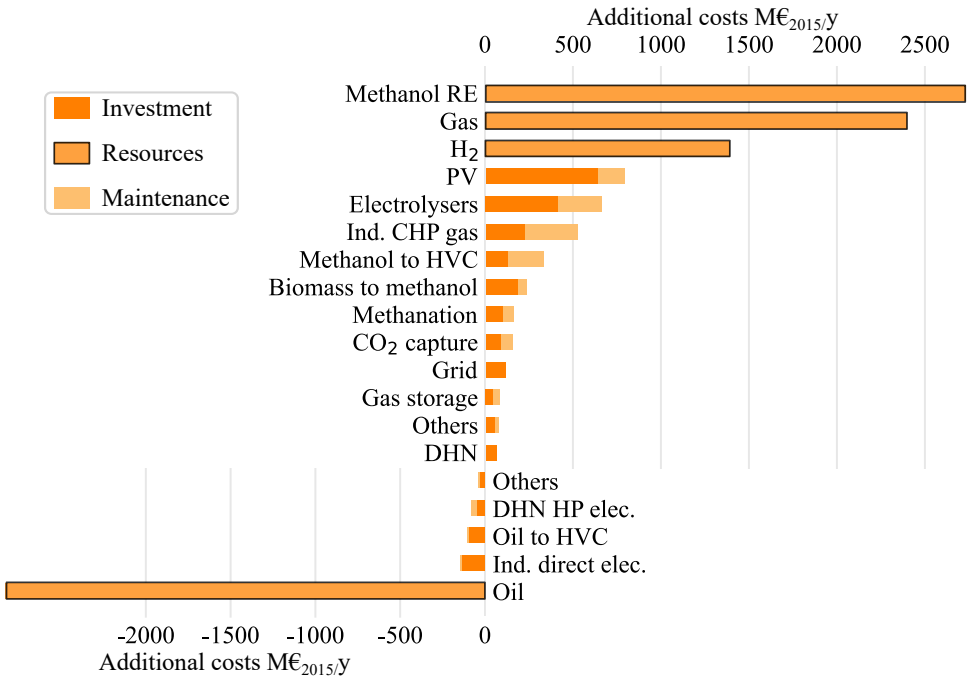

Figure D.2: The breakdown of the additional costs relative to the case with no power-to-gas indicates the origins of the 6.3 b€$_{2015}$/y difference of total cost. Abbreviations: renewable (RE), industrial (ind.), combined heat and power (CHP), high-value chemicals (HVC), photovoltaic (PV).

D.3 Sensitivity of the total cost

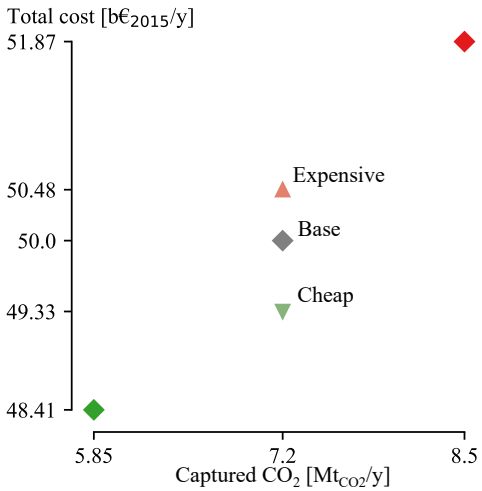

Figure D.3: The uncertainty related to the quantity of captured CO_2 leads to a variation of +3.7% and -3.2% of the total cost, which is more than with the technologies costs on the lower limit (cheap scenario) and the upper limit (expensive scenario). The total cost corresponds to the full utilisation of the CO_2 captured by oxy-fuel combustion capture. All the diamond markers refer to the base costs.

Bibliography

[1] IPCC, "Climate change 2021: The physical science basis. contribution of working group i to the sixth assessment report of the intergovernmental panel on climate change," *Cambridge University Press*, pp. 3–32, 2021. doi: 10.1017/9781009157896.001.

[2] UNFCC, *The paris agreement*, Government Document, 2015. [Online]. Available: http://unfccc.int/paris_agreement/items/9485.php.

[3] IEA, "World energy statistics and balances," 2023. [Online]. Available: https://www.iea.org/data-and-statistics/data-product/world-energy-statistics-and-balances.

[4] Global CCS Institute, "The global status of ccs: 2020," Report, 2020.

[5] European Climate, Infrastructure and Environment Executive Agency, "Pioneering port aiming at net zero by 2050," 2023. [Online]. Available: https://cinea.ec.europa.eu/news-events/news/pioneering-port-aiming-net-zero-2050-2023-03-03_en.

[6] Port of Antwerp Bruges, "Antwerp@c," [Online]. Available: https://www.portofantwerpbruges.com/en/our-port/climate-and-energy-transition/antwerpc.

[7] D. Y. C. Leung, G. Caramanna, and M. M. Maroto-Valer, "An overview of current status of carbon dioxide capture and storage technologies," *Renewable and Sustainable Energy Reviews*, vol. 39, pp. 426–443, 2014, issn: 1364-0321. doi: 10.1016/j.rser.2014.07.093.

[8] C. Songa, Q. Liua, S. Dengb, H. Lic, and Y. Kitamurad, "Cryogenic-based co2 capture technologies: State-of-the-art developments and current challenges," *Renewable and Sustainable Energy Reviews*, vol. 101, pp. 265–278, 2019, issn: 1364-0321. doi: 10.1016/j.rser.2018.11.018.

[9] R. Allam *et al.*, "Capture of co2," in *IPCC Special Report on Carbon Dioxide Capture and Storage*, B. Metz, O. Davidson, H. de Coninck, M. Loos, and L. Meyer, Eds. UK: Cambridge University Press, 2005, pp. 105–179.

[10] D. Jansen, M. Gazzani, G. Manzolini, E. v. Dijk, and M. Carbo, "Pre-combustion co2 capture," *International Journal of Greenhouse Gas Control*, vol. 40, pp. 167–187, 2015, issn: 1750-5836. doi: 10.1016/j.ijggc.2015.05.028.

[11] M. Kheirinik, S. Ahmed, and N. Rahmanian, "Comparative techno-economic analysis of carbon capture processes: Pre-combustion, post-combustion, and oxy-fuel combustion operations," *Sustainability*, vol. 13, *24*, p. 13 567, 2021, issn: 2071-1050. doi: 10.3390/su132413567.

[12] M. Wang, A. Lawal, P. Stephenson, J. Sidders, and C. Ramshaw, "Post-combustion co2 capture with chemical absorption: A state-of-the-art review," *Chemical Engineering Research and Design*, vol. 89, *9*, pp. 1609–1624, 2011, issn: 0263-8762. doi: 10.1016/j.cherd.2010.11.005.

[13] E. Koohestanian and F. Shahraki, "Review on principles, recent progress, and future challenges for oxy-fuel combustion co2 capture using compression and purification unit," *Journal of Environmental Chemical Engineering*, vol. 9, *4*, p. 105 777, 2021, issn: 2213-3437. doi: 10.1016/j.jece.2021.105777.

[14] F. Normann, *Oxy-Fuel Combustion - The Control of Nitrogen Oxides*. Göteborg, Sweden, 2010, isbn: 978-91-7385-401-6.

[15] R. Stanger *et al.*, "Oxyfuel combustion for co2 capture in power plants," *International Journal of Greenhouse Gas Control*, vol. 40, pp. 55–125, 2015, issn: 1750-5836. doi: 10.1016/j.ijggc.2015.06.010.

[16] M. A. Nemitallah, M. A. Habib, H. M. Badr, S. A. Said, A. Jamal, R. Ben-Mansour, E. M. A. Mokheimer, and K. Mezghani, "Oxy-fuel combustion technology: Current status, applications, and trends," *International Journal of Energy Research*, vol. 41, *12*, pp. 1670–1708, 2017, issn: 0363-907X. doi: 10.1002/er.3722.

[17] T. Kuramochi, A. Ramírez, W. Turkenburg, and A. Faaij, "Comparative assessment of co2 capture technologies for carbon-intensive industrial processes," *Progress in Energy and Combustion Science*, vol. 38, *1*, pp. 87–112, 2012, issn: 0360-1285. doi: 10.1016/j.pecs.2011.05.001.

[18] S. García-Luna, C. Ortiz, A. Carro, R. Chacartegui, and L. A. Pérez-Maqueda, "Oxygen production routes assessment for oxy-fuel combustion," *Energy*, vol. 254, p. 124 303, 2022, issn: 0360-5442. doi: 10.1016/j.energy.2022.124303.

[19] C.-H. Yu, C.-H. Huang, and C.-S. Tan, "A review of co2 capture by absorption and adsorption," *Aerosol and Air Quality Research*, vol. 12, *5*, pp. 745–769, 2012, issn: 1680-8584. doi: 10.4209/aaqr.2012.05.0132.

[20] S. D. Kenarsari, D. Yang, G. Jiang, S. Zhang, J. Wang, A. G. Russell, Q. Wei, and M. Fan, "Review of recent advances in carbon dioxide separation and capture," *RSC Advances*, vol. 3, *45*, pp. 22 739–22 773, 2013. doi: 10.1039/C3RA43965H.

[21] R. Saxena, V. K. Singh, and E. A. Kumar, "Carbon dioxide capture and sequestration by adsorption on activated carbon," *Energy Procedia*, vol. 54, pp. 320–329, 2014, issn: 1876-6102. doi: 10.1016/j.egypro.2014.07.275.

[22] Z. Dai, R. D. Noble, D. L. Gin, X. Zhang, and L. Deng, "Combination of ionic liquids with membrane technology: A new approach for co2 separation," *Journal of Membrane Science*, vol. 497, pp. 1–20, 2016, issn: 0376-7388. doi: 10.1016/j.memsci.2015.08.060.

[23] M. Bailera, N. Kezibri, L. M. Romeo, S. Espatolero, P. Lisbona, and C. Bouallou, "Future applications of hydrogen production and co2 utilization for energy storage: Hybrid power to gas-oxycombustion power plants," *International Journal of Hydrogen Energy*, vol. 42, *19*, pp. 13 625–13 632, 2017, issn: 0360-3199. doi: 10.1016/j.ijhydene.2017.02.123.

[24] European Environment Agency. "Industrial reporting under the industrial emissions directive 2010/75/eu and european pollutant release and transfer register regulation (ec) no 166/2006." (2022), [Online]. Available: hhttps://www.eea.europa.eu/data-and-maps/data/industrial-reporting-under-the-industrial-7.

[25] J. Liu *et al.*, "Carbon and air pollutant emissions from china's cement industry 1990–2015: Trends, evolution of technologies, and drivers," *Atmospheric Chemistry and Physics*, vol. 21, *3*, pp. 1627–1647, 2021, issn: 1680-7324. doi: 10.5194/acp-21-1627-2021. [Online]. Available: http://gidmodel.org.cn/.

[26] D. Tong *et al.*, *Targeted emission reductions from global super-polluting power plant units*, Dataset, 2018. [Online]. Available: http://gidmodel.org.cn/.

[27] X. Wang, Y. Lei, L. Yan, T. Liu, Q. Zhang, and K. He, "A unit-based emission inventory of so2, nox and pm for the chinese iron and steel industry from 2010 to 2015," *Science of The Total Environment*, vol. 676, pp. 18–30, 2019, issn: 0048-9697. [Online]. Available: http://gidmodel.org.cn/.

[28] L. Bourgeois *et al.*, *EU refinery energy systems and efficiency*. Brussels: Concawe, 2012. [Online]. Available: https://www.concawe.eu/wp-content/uploads/2017/01/rpt_12-03-2012-01520-01-e.pdf.

[29] Fluxys. "Our infrastructure." (2023), [Online]. Available: https://www.fluxys.com/en/about-us/fluxys-belgium/infrastructure (visited on 05/21/2023).

[30] Fluxys, "H2/co2 quality specifications proposals," Report, 2021.

[31] R. Chauvy, D. Verdonck, L. Dubois, D. Thomas, and G. De Weireld, "Techno-economic feasibility and sustainability of an integrated carbon capture and conversion process to synthetic natural gas," *Journal of CO2 Utilization*, vol. 47, 2021, issn: 2212-9820. doi: 10.1016/j.jcou.2021.101488.

[32] S. E. Ul Haq, F. Uddin, S. A. A. Taqvi, M. Naqvi, and S. R. Naqvi, "Multistage carbon dioxide compressor efficiency enhancement using waste heat powered absorption chillers," *Energy Science & Engineering*, vol. 9, *9*, pp. 1373–1384, 2021, optimum compression ratio, issn: 2050-0505. doi: 10.1002/ese3.898.

[33] S. Chen, Y. Zheng, M. Wu, J. Hu, and W. Xiang, "Thermodynamic analysis of oxy-fuel combustion integrated with the sco2 brayton cycle for combined heat and power production," *Energy Conversion and Management*, vol. 232, p. 113 869, 2021, issn: 0196-8904. doi: 10.1016/j.enconman.2021.113869.

[34] G. Limpens, *Generating energy transition pathways: application to Belgium*. 2021. doi: 10.13140/RG.2.2.25755.18724.

[35] IRENA, "Hydrogen," 2022. [Online]. Available: https://www.irena.org/Energy-Transition/Technology/Hydrogen.

[36] A. Buttler and H. Spliethoff, "Current status of water electrolysis for energy storage, grid balancing and sector coupling via power-to-gas and power-to-liquids: A review," *Renewable and Sustainable Energy Reviews*, vol. 82, pp. 2440–2454, 2018, issn: 1364-0321. doi: 10.1016/j.rser.2017.09.003.

[37] J. B. Hansen, "Solid oxide electrolysis – a key enabling technology for sustainable energy scenarios," *Faraday Discussions*, vol. 182, *0*, pp. 9–48, 2015, issn: 1359-6640. doi: 10.1039/C5FD90071A.

[38] A. Brisse, J. Schefold, and M. Zahid, "High temperature water electrolysis in solid oxide cells," *International Journal of Hydrogen Energy*, vol. 33, *20*, pp. 5375–5382, 2008, issn: 0360-3199. doi: 10.1016/j.ijhydene.2008.07.120.

[39] M. Carmo, D. L. Fritz, J. Mergel, and D. Stolten, "A comprehensive review on pem water electrolysis," *International Journal of Hydrogen Energy*, vol. 38, *12*, pp. 4901–4934, 2013, issn: 0360-3199. doi: 10.1016/j.ijhydene.2013.01.151.

[40] K. Zeng and D. Zhang, "Recent progress in alkaline water electrolysis for hydrogen production and applications," *Progress in Energy and Combustion Science*, vol. 36, *3*, pp. 307–326, 2010, issn: 0360-1285. doi: 10.1016/j.pecs.2009.11.002.

[41] IEA, "Electrolysers," *IEA*, 2022. [Online]. Available: https://www.iea.org/reports/electrolysers.

[42] Cummins, *Hylyzer®water electrolyzers*, Catalog, 2021. [Online]. Available: https://www.cummins.com/sites/default/files/2021-08/cummins-hylyzer-1000-specsheet.pdf.

[43] Port of Antwerp Bruges. "Water," [Online]. Available: https://www.portofantwerpbruges.com/en/our-port/people-and-environment/clean-port/water.

[44] D. Burrin, S. Roy, A. P. Roskilly, and A. Smallbone, "A combined heat and green hydrogen (chh) generator integrated with a heat network," *Energy Conversion and Management*, vol. 246, p. 114 686, 2021, issn: 0196-8904. doi: 10.1016/j.enconman.2021.114686.

[45] S. Brynolf, M. Taljegard, M. Grahn, and J. Hansson, "Electrofuels for the transport sector: A review of production costs," *Renewable and Sustainable Energy Reviews*, vol. 81, pp. 1887–1905, 2018, Insane doc for costs of the diff tech + efficiencies, issn: 1364-0321. doi: 10.1016/j.rser.2017.05.288.

[46] J. Gorre, F. Ortloff, and C. van Leeuwen, "Production costs for synthetic methane in 2030 and 2050 of an optimized power-to-gas plant with intermediate hydrogen storage," *Applied Energy*, vol. 253, p. 113 594, 2019, issn: 0306-2619. doi: 10.1016/j.apenergy.2019.113594.

[47] IEA, "The future of hydrogen," 2019. [Online]. Available: https://www.iea.org/reports/the-future-of-hydrogen.

[48] G. Palmer, A. Roberts, A. Hoadley, R. Dargaville, and D. Honnery, "Life-cycle greenhouse gas emissions and net energy assessment of large-scale hydrogen production via electrolysis and solar pv," *Energy & Environmental Science*, vol. 14, *10*, pp. 5113–5131, 2021, issn: 1754-5692. doi: 10.1039/D1EE01288F.

[49] S. Rönsch, J. Schneider, S. Matthischke, M. Schlüter, M. Götz, J. Lefebvre, P. Prabhakaran, and S. Bajohr, "Review on methanation – from fundamentals to current projects," *Fuel*, vol. 166, pp. 276–296, 2016, issn: 0016-2361. doi: 10.1016/j.fuel.2015.10.111.

[50] K. Ghaib, K. Nitz, and F.-Z. Ben-Fares, "Chemical methanation of co2: A review," *ChemBioEng Reviews*, vol. 3, *6*, pp. 266–275, 2016, issn: 2196-9744. doi: 10.1002/cben.201600022.

[51] J. Gao, Q. Liu, F. Gu, B. Liu, Z. Zhong, and F. Su, "Recent advances in methanation catalysts for the production of synthetic natural gas," *RSC Advances*, vol. 5, *29*, pp. 22 759–22 776, 2015, issn: 2046-2069. doi: 10.1039/c4ra16114a.

[52] P. Melo Bravo and D. P. Debecker, "Combining co2 capture and catalytic conversion to methane," *Waste Disposal & Sustainable Energy*, vol. 1, *1*, pp. 53–65, 2019, issn: 2524-7980. doi: 10.1007/s42768-019-00004-0.

[53] D. Coppitters, A. Costa, R. Chauvy, L. Dubois, W. De Paepe, D. Thomas, G. De Weireld, and F. Contino, "Energy, exergy, economic and environmental (4e) analysis of integrated direct air capture and co2 methanation under uncertainty," *Fuel*, vol. 344, p. 127 969, 2023, issn: 0016-2361. doi: 10.1016/j.fuel.2023.127969.

[54] J. Gorre, F. Ruoss, H. Karjunen, J. Schaffert, and T. Tynjälä, "Cost benefits of optimizing hydrogen storage and methanation capacities for power-to-gas plants in dynamic operation," *Applied Energy*, vol. 257, p. 113 967, 2020, issn: 0306-2619. doi: 10.1016/j.apenergy.2019.113967.

[55] J. Ma, L. Li, H. Wang, Y. Du, J. Ma, X. Zhang, and Z. Wang, "Carbon capture and storage: History and the road ahead," *Engineering*, vol. 14, pp. 33–43, 2022, issn: 2095-8099. doi: 10.1016/j.eng.2021.11.024.

[56] Parlement bruxellois, *Projet d'ordonnance*, Government Document, 2021. [Online]. Available: http://weblex.brussels/data/crb/doc/2021-22/143112/images.pdf.

[57] R. Svensson, M. Odenberger, F. Johnsson, and L. Strömberg, "Transportation systems for co2—application to carbon capture and storage," *Energy Conversion and Management*, vol. 45, *15*, pp. 2343–2353, 2004, issn: 0196-8904. doi: 10.1016/j.enconman.2003.11.022.

[58] T. Vangkilde-Pedersen, "Eu geocapacity: Assessing european capacity for geological storage of carbon dioxide," Report, 2008.

[59] H. Bolscher *et al.*, "High level report: Ccus in europe," Report, 2019.

[60] K. Welkenhuysen, K. Piessens, J.-M. Baele, B. Laenen, and M. Dusar, "Co2 storage opportunities in belgium," *Energy Procedia*, vol. 4, pp. 4913–4920, 2011, issn: 1876-6102. doi: 10.1016/j.egypro.2011.02.460.

[61] Fluxys, "Information memorandum for co2 infrastructure," Report, 2022.

[62] Fluxys, *Antwerp export hub*, 2023. [Online]. Available: https://www.fluxys.com/en/projects/antwerp-export-hub (visited on 05/30/2023).

[63] Northern Lights, *What we do*, 2023. [Online]. Available: https://norlights.com/ (visited on 05/30/2023).

[64] European Commission, "Co2 transports aims to establish infrastructure to facilitate large-scale capture, transport and storage of co2 from rotterdam, antwerp and the north sea port," Report, 2023.

[65] P.-Y. Oei, J. Herold, and R. Mendelevitch, "Modeling a carbon capture, transport, and storage infrastructure for europe," *Environmental Modeling and Assessment*, vol. 19, pp. 515–531, 2014. doi: 10.1007/s10666-014-9409-3.

[66] K. Lauri, R. Jouko, N. Nicklas, and T. Sebastian, "Scenarios and new technologies for a north-european co2 transport infrastructure in 2050," *Energy Procedia*, vol. 63, pp. 2738–2756, 2014, issn: 1876-6102. doi: 10.1016/j.egypro.2014.11.297.

[67] European Commission. "Industrial emissions directive." (2023), [Online]. Available: https://environment.ec.europa.eu/topics/industrial-emissions-and-safety/industrial-emissions-directive_en (visited on 05/30/2023).

[68] Gouvernement belge, *Plan National pour la reprise et la résilience*. Bruxelles: Cabinet du Secrétaire d'Etat à la Relance et aux Investissements Stratégiques, en charge de la Politique Scientifique., 2021.

[69] Belgian federal government, "Vision and strategy hydrogen," Report, 2022.

[70] H. Ritchie, M. Roser, and P. Rosado, "Co□ and greenhouse gas emissions," *Our World in Data*, 2020. [Online]. Available: https://ourworldindata.org/co2-and-greenhouse-gas-emissions.

[71] S. Werner, *European District Heating Price Series*. 2016, isbn: 978-91-7673-316-5.

[72] R. C. Pietzcker, S. Osorio, and R. Rodrigues, "Tightening eu ets targets in line with the european green deal: Impacts on the decarbonization of the eu power sector," *Applied Energy*, vol. 293, p. 116 914, 2021, issn: 0306-2619. doi: 10.1016/j.apenergy.2021.116914.

[73] Bloomberg Finance L.P, *EUETSSY1 Index*, Dataset. (visited on 08/02/2023).

[74] European Commission, "Eu reference scenario 2016: Energy, transport and ghg emissions trends to 2050," 2016.

[75] J. Yates, R. Daiyan, R. Patterson, R. Egan, R. Amal, A. Ho-Baille, and N. L. Chang, "Techno-economic analysis of hydrogen electrolysis from off-grid stand-alone photovoltaics incorporating uncertainty analysis," *Cell Reports Physical Science*, vol. 1, *10*, p. 100 209, 2020, issn: 2666-3864. doi: 10.1016/j.xcrp.2020.100209.

[76] C. van Leeuwen and A. Zauner, "Innovative large-scale energy storage technologies and power-to-gas concepts after optimisation," *Report on the costs involved with PtG technologies and their potentials across the EU, University of Groningen*, 2018.

[77] European commission, "Eu solar energy strategy," 2022.

[78] B. Van Speybroeck and W. Peter, *11 mois après les inondations, près de 90% des sinistrés ont été indemnisés*, Newspaper Article, 2022. [Online]. Available: http://prez.ly/Wgec.

[79] European Commission, *Communication from the commission to the European parliament, the council, the European economic and social committee and the committee of the regions on the European hydrogen bank*. Brussels, 2023.

[80] Chemical Engineering. "Chemical engineering's plant cost index," [Online]. Available: https://www.chemengonline.com/pci-home (visited on 04/01/2023).

UNIVERSITÉ CATHOLIQUE DE LOUVAIN
École polytechnique de Louvain
Rue Archimède, 1 bte L6.11.01, 1348 Louvain-la-Neuve, Belgique | **www.uclouvain.be/epl**